Celestial Mechanics and Dynamical Astronomy (2020) 132:47
https://doi.org/10.1007/s10569-020-09986-0

ORIGINAL ARTICLE

The precession and nutations of a rigid Mars

Rose-Marie Baland[1] · Marie Yseboodt[1] · Sébastien Le Maistre[1] · Attilio Rivoldini[1] · Tim Van Hoolst[1] · Véronique Dehant[1]

Received: 13 January 2020 / Revised: 13 June 2020 / Accepted: 28 August 2020

Abstract
The nutations of Mars are about to be estimated to a few milliarcseconds accuracy with the radioscience experiments onboard InSight and ExoMars 2022. The contribution to the nutations due to the liquid core and tidal deformations will be detected, allowing to constrain the interior of Mars. To avoid introducing systematic errors in the determination of the core properties, an accurate precession and nutation model for a rigidly behaving Mars is needed. Here, we develop such a model with adequate accuracy based on the Torque approach and compare it to previous models. We include in the model the forcings by the Sun, Phobos, Deimos, and the other planets of the solar system. We also include the geodetic precession and nutations. We use semi-analytical developments for the solar and planetary torques, and analytical solutions for the effect of Phobos and Deimos and for the geodetic precession and nutations. With a truncation criterion of 0.025 milliarcseconds in prograde and/or retrograde amplitude, we identify 43 nutation terms. The uncertainty on our solution mainly derives from the observational uncertainty on the current determination of the precession rate of Mars. Uncertainties related to our modeling choices are negligible in comparison. Given the current determination of the precession rate (7608.3 $\pm$ 2.1 mas/yr, Konopliv et al. in Icarus 274:253–260, 2016. https://doi.org/10.1016/j.icarus.2016.02.052), our model predicts a dynamical flattening $H_D = 0.00538017 \pm 0.00000148$ and a normalized polar moment of inertia $C/\mathrm{MR}^2 = 0.36367 \pm 0.00010$ for Mars.

Keywords Nutation · Precession · Mars

1 Introduction

The geodesy experiments Rotation and Interior Structure Experiment (RISE, Folkner et al. 2018) and Lander Radioscience (LaRa, Dehant et al. 2020) on InSight and ExoMars 2022 measure the rotation of Mars by tracking the respective lander on its surface. From the measurements, important orientation parameters of Mars are determined. These are the length-of-day variations, the polar motion of the spin axis with respect to a crust-fixed frame, and the precession/nutation of the spin axis in space.

✉ Rose-Marie Baland
rose-marie.baland@oma.be

[1] Royal Observatory of Belgium, Ringlaan 3, 1180 Brussels, Belgium

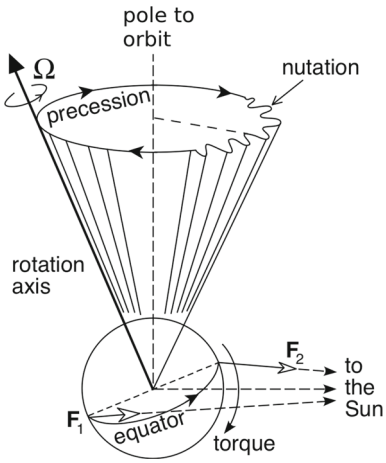

Fig. 1 Precession and nutations of the spin axis about the orbit pole. Adapted from Lowrie (2011)

The precession is the slow uniform circular retrograde motion of the spin axis about the perpendicular to the orbital plane induced mainly by the gravitational torque exerted by the Sun on Mars, which reacts as a spinning top (see Fig. 1). The aperture of the precession cone is about 25° and the precession period is about 170,000 years, corresponding to the rate of -7608.3 ± 2.1 mas/yr (milliarcsecond per year, Konopliv et al. 2016). The precession rate is, on the one hand, proportional to the J_2 gravity coefficient (a spherical planet would not precess) which is well known from gravity field measurements, and, on the other hand, inversely proportional to the polar moment of inertia C which constrains interior models of Mars (e.g., Rivoldini et al. 2011).

The nutations are short-period (e.g., the revolution period of Mars and its harmonics) oscillations of the orientation of the spin axis with amplitudes reaching a few hundreds milliarcseconds (mas). Note that 1 mas corresponds to a displacement of 1.6 cm at the surface of Mars. The nutations are superimposed on the precession, so that the spin axis trajectory in space appears wiggly. Nutations occur mainly because of periodical changes in the solar torque during the orbital motion of Mars. Additionally, the torques exerted by the other planets of the solar system and by Phobos and Deimos, the two natural satellites of Mars, contribute to the nutations.

The tides raised on Mars by the Sun indicate that Mars has an internal liquid core (Yoder et al. 2003), with a radius between about 1730 and 1860 km (Rivoldini et al. 2011; Khan et al. 2018). A planet with a liquid core is characterized by a rotational normal mode called *Free Core Nutation* (FCN) that depends on its interior properties (core radius and shape, capacity to deform) and that can resonantly amplify nutations (e.g., Hilton 1992; Groten et al. 1996; Folkner et al. 1997a). In the frequency domain, nutation amplitudes are conveniently expressed by multiplying *rigid nutation* amplitudes with a *transfer function* (e.g., Folkner et al. 1997a, after Sasao et al. 1980). The rigid nutations represent the nutations of an entirely solid and rigid planet of given mass and moments of inertia. The transfer function depends on the precise interior structure and allows to account for the effect of the fluid core as well as for the tidal deformations. The effect of the transfer function on the prograde semi-annual nutation (whose amplitude is often denoted p_2), the largest nutation, ranges between 5 and 25 mas, depending on the free core nutation period. The retrograde ter-annual nutation (r_3) can be enhanced by a few tens of mas in the presence of a large liquid core (Dehant et al. 2000; Le Maistre et al. 2012, 2020).

The model of Mars rotation used for radioscience data analysis usually includes precession and nutation (e.g., Folkner et al. 1997b; Kuchynka et al. 2014; Konopliv et al. 2016). Whereas the precession rate can be estimated from the data, the main nutation terms are held fixed to values obtained from a rigid nutation model and a transfer function, because they cannot be determined with a satisfying accuracy from the data. For example, in the analysis of the radio signals exchanged with Viking lander 1 by Borderies et al. (1980), the main nutation terms have been determined with large uncertainties (50–100% level). Le Maistre (2013) and Le Maistre et al. (2018) used historical data from several landed missions (Viking lander 1, Pathfinder, the Mars Exploration Rovers Spirit and Opportunity) to determine the amplitudes of the main nutation terms. However, the transfer function contribution was difficult to determine with a sufficient precision to constrain interior models of Mars. RISE and LaRa will further improve the determination of the main nutation terms of Mars. The expected precision on p_2 and r_3 measurements with LaRa alone lies between 2 and 15 mas, depending on the mission operational parameters (Le Maistre et al. 2020). The uncertainties reduce by 2–3 mas when using both RISE and LaRa data together (Dehant et al. 2020; Péters et al. 2020). The expected precision is sufficient to provide an independent assessment of the state of the core as well as a constraint on the core radius that can be comparable to that obtained by the Love number k_2, depending on the period of the FCN. Additionally, nutation can also constrain the shape of the core.

In order to infer reliable properties about the core from the forthcoming radioscience data, an accurate model for the precession/nutation of a rigid Mars is needed. The first detailed rigid precession/nutation model has been proposed during the operational period of the Viking landers (Reasenberg and King 1979). The most recent rigid precession/nutation models date from 20 years ago (Bouquillon and Souchay 1999; Roosbeek 1999). In this study, our aim is twofold. As the differences between the existing models are large, we assess their accuracy. At the same time, we determine the most efficient and accurate method to provide an up to date rigid precession/nutation model consistent with the latest orbital ephemerides of the bodies of the solar system, in order to prepare the analysis of the forthcoming radioscience data.

The plan of the paper is as follows. In Sect. 2, we present the existing models for the precession and nutations of a rigid Mars and we compare them to each other. In Sect. 3, we introduce the governing equations and we derive approximated analytical solutions for the precession and nutations due to the Sun, Phobos and Deimos, and the other planets. This allows to better understand the strengths and weaknesses of the existing approaches, but also what differentiates them. We chose the approach of Roosbeek (1999), simple to implement and sufficiently accurate in comparison to the precision on future measurements, to generate an up-to-date solution for the precession and nutations of a rigid Mars in Sect. 4. But before that, we recompute the series of Roosbeek (1999), named RMAN99 for Roosbeek Martian Analytical Nutations 1999, with modern computer performances and, as a result, find significant differences with respect to the original series. The recomputed RMAN99 series is necessary to correctly assess the changes introduced when updating the series. By analogy, the updated version of the precession/nutations series will be called BMAN20 for Baland Martian Analytical Nutations 2020. A simplified version more suited for the interpretation of radioscience data (BMAN20RS) is also provided. In Sect. 5, we examine the definition of the IAU standard for Mars right ascension and declination. We end with a discussion and concluding remarks in Sect. 6.

2 Current status of precession and nutations of a rigid Mars

2.1 Initial results

To provide the means for analyzing data from the Viking landers and future lander missions, Reasenberg and King (1979) (**RK79** hereafter) developed a rotation model of a rigid Mars including both the precession and nutation terms. Their goal was to identify all the precession terms down to 0.14 mas/yr, corresponding to a surface displacement of at least 1 cm in a 10-year period, and the nutation terms with amplitudes down to about 0.7 mas in longitude and 0.3 mas in obliquity, corresponding to peak-to-peak displacements of 1 cm.

They considered the torque exerted by the Sun on an axisymmetric and flattened Mars evolving on a precessing elliptic orbit. They found a theoretical precession rate of -7568 mas/yr and nutation terms with frequencies equal to harmonics of the mean motion of Mars (the *main solar terms* hereafter). Given the considered truncation criterion, they included terms up to the sixth harmonic in their solution (the same year, Lyttleton et al. 1979 published a solution with terms up to the fourth harmonic). The non-axial symmetry of Mars leads to semi-diurnal nutation with an amplitude of the order of 0.1 mas, below the truncation criterion. RK79 included in their model a geodetic precession of 6.70 mas/yr resulting from general relativity. Regarding the direct torques by the other planets, the effect of Jupiter was introduced as a small additional contribution of -0.22 mas/yr to the precession rate.

The RK79 nutation series are elegantly written in a simple form using only two arguments. The first argument, denoted M, is the mean anomaly of Mars. The second argument, denoted q, is twice the pericenter longitude of the Sun measured from the node of the Body Frame (BF) on the orbit of Mars. This argument is obtained as $q = 2\omega - 2\theta$, with ω the argument of perihelion of Mars measured from the node of Mars orbit on the ecliptic of the Earth and θ the angle between the two aforementioned nodes, see Fig. 4. The simplicity of RK79 nutations series explains why they are still considered nowadays for computing the rotation model used to analyze radioscience data from recent missions (e.g., Kuchynka et al. 2014; Konopliv et al. 2016), as well as for defining the IAU model for Mars orientation (Kuchynka et al. 2014; Archinal et al. 2018). However, RK79 do not include the nutations induced by the direct torques by Phobos and Deimos (the *satellite terms* hereafter). These nutations are large (up to 10 mas in longitude, as demonstrated later) and should be included in Mars rotation model. Several smaller and neglected effects will also have to be considered in view of the precision expected with RISE and LaRa. In particular, we will consider the effect of the modifications of the solar torque due to the perturbations of the orbit of Mars by the other planets (the *indirect planetary terms*), as well as the effect of the direct torques by the other planets (the *direct planetary terms*).

Over the next two decades, other authors (Borderies 1980; Borderies et al. 1980; Hilton 1991; Groten et al. 1996) proposed a solution for the precession and nutations of a rigid Mars. A common feature of these studies is the computation of the main solar terms of the nutations assuming that Mars is axisymmetric and evolves on a Keplerian orbit of a given eccentricity. The series of Borderies (1980) are not directly comparable to those of RK79, due to a different choice of reference plane (the Earth ecliptic versus Mars orbit). The series of Borderies et al. (1980), Hilton (1991) and Groten et al. (1996) are comparable to RK79 series: the orbit of Mars is chosen as the reference plane and the set of arguments are equivalent.[1] Their truncation criterion was larger or similar, leading to less or about the same number

[1] The arguments $2\omega - 2h$ of Borderies (h is the same angle as the angle θ defined above), 2Λ of Hilton, and $2\Phi_0$ of Groten correspond by definition to the argument q of RK79. Note that a confusion between the

of solar terms as in RK79. It results that none of those series is good enough to supersede those of RK79. Yet, their authors explored other aspects of the problem that can impact the interpretation of radioscience data, laying the foundations for subsequent studies. For instance, Hilton (1991) was the first to recognize the importance of the effects of Phobos and Deimos (see Sect. 3.5 for more details). He also investigated the direct effects of the other planets (see Sect. 3.6). Groten et al. (1996) noticed that the nutation amplitudes may change with time because of the secular variations in the eccentricity[2] and perihelion of the orbit of Mars due to perturbations by the other planets (the reasoning is extended to the effect of the other orbital elements in Sect. 3.4.2).

2.2 Roosbeek, Bouquillon, and Souchay

To the best of our knowledge, Roosbeek (1999) and Bouquillon and Souchay (1999) (**RMAN99** and **BS99** hereafter) published the most recent and detailed solutions for the precession and nutation of a rigid Mars. These studies already date from 20 years ago. The methodologies of the two studies differ from each other: BS99 is based on the Hamiltonian approach (i.e., working with the Hamiltonian corresponding to the total energy of the system), whereas RMAN99 considers the Torque approach (i.e., working with the gravitational torque acting on Mars). Besides the solar terms (main solar terms and indirect planetary terms), RMAN99 and BS99 also include the satellite terms in their solution. Some direct planetary terms (induced by the Earth and Jupiter) are included in BS99, but not in RMAN99.

Their main improvement compared to previous studies lies in the modeling of the planets' motion. RMAN99 abandoned the Keplerian representation of the orbit of Mars and the use of mean orbital elements, and considered instead the rectangular coordinates and distance to the Sun as given by a semi-analytical theory for planetary ephemerides called VSOP87 (Bretagnon and Francou 1988). The acronym VSOP stands for *Variations Séculaires des Orbites planétaires* (Secular Variations of Planetary Orbits). As a consequence, the model provides a semi-analytical description of the precession/nutations, instead of the analytical description in terms of the mean orbital elements provided in RK79. Unlike RMAN99, BS99 considered an approach partially based on the VSOP87 ephemerides, and partially on the assumption of osculating orbits.[3]

numerical values of $\omega - \theta$ and ω in Groten et al. (1996) (he wrongly uses $q = -147°$ instead of $q \cong 142°$) renders his series incorrect.

[2] Hilton (1991) also attempted to take into account the changes in eccentricity with time. He wrongly assumed that the orbit perturbations change the J2000 mean eccentricity (e_0), leading to incorrect changes in the precession rate and mean values of the nutation amplitudes. The eccentricity is defined as $e = \sqrt{h^2 + k^2}$ with h and k given in Bretagnon (1982) under the form $\sum_n h_n$ and $\sum_n k_n$, see Eq. (57) of Hilton (1991). When we follow his procedure to extract the J2000 mean eccentricity, we find $e_0 = 0.0936037$, whereas $e_0 = 0.0934006$, see Simon et al. (1994). As a consequence, the term in $\sin M$ in his Table 1 with an amplitude of -634.4 mas and which is proportional to e_0 is wrongly changed by 1.4 mas, see his Table 2. What is wrong in Hilton's procedure? First, he constructs the eccentricity as $e = \sum_n \sqrt{h_n^2 + k_n^2} = \sum_n e_n$ instead of $\sqrt{(\sum_n h_n)^2 + (\sum_n k_n)^2}$. Second, he expands each e_n about $T = 0$ and keeps the zeroth-order terms, which makes no sense for relatively short period terms (between 400 and 6000 days for the principal terms of h and k). The correct value of e_0 can be obtained by expanding $\sqrt{(\sum_n h_n)^2 + (\sum_n k_n)^2}$ about $\sqrt{h_0^2 + k_0^2}$ with h_0 and k_0 the constant parts of h and k.

[3] For the gravitational action of the Sun, the factor $1/r^3$ in their disturbing potential U_i (their Eq. 7), with r the distance of the Sun to Mars, is developed as a function of the eccentricity and mean longitude of Mars,

The use of accurate planetary ephemerides, as VSOP87, which accounts for their mutual perturbations,[4] affects the precession/nutation model in two ways. First, provided that the truncation criterion is small enough, nutation terms with frequencies other than the harmonics of the mean motion of Mars, the indirect planetary terms, appear in addition to the main solar terms, as shown in RMAN99 and BS99. Second, they produce secular changes in the nutation amplitudes,[5] as demonstrated in BS99 (their *mixed terms*). The latter effect was overlooked in RMAN99.

Both RMAN99 and BS99 provide series for the nutations in longitude and obliquity choosing a truncation criterion of 0.1 mas in amplitude, below that of RK79. This truncation level is not the level of precision on the amplitude of a given nutation term, which also depends on the precision of the choice of ephemerides and parameter values, modeling assumptions, and computer limitations.[6] As a matter of fact, the agreement between RMAN99 and BS99, term by term, is at the mas level, an order of magnitude above the truncation level (up to 2 mas for the semi-annual solar and Phobos terms in longitude, see Table 1). In the time domain, the cumulated difference between the two series can reach 6 mas in longitude and 2 mas in obliquity, as can be seen in panels (a, b) of Fig. 2. Such large differences are unexpected since both series are based on the same ephemerides (VSOP87 for the planets and ESAPHO and ESADE for Phobos and Deimos, see Chapront-Touze 1990) and are too large to be ignored, as the effect of the fluid core on the nutation amplitude can be of that order.

Some difference results from different values used for the mass of Phobos $\mathcal{M}_{Ph}$ and the *scaling factor* H_D. As demonstrated in Sect. 3.2, Eq. (11c), the scaling factor is defined as the ratio of the difference between the polar and the mean equatorial moments of inertia over the polar moment of inertia $(C - \bar{A})/C$ and contributes to the amplitude of each term in the nutations series. H_D is taken as 0.00535464 in RMAN99[7] and as 0.005363 in BS99. The value of Phobos mass in BS99 is 22% larger than the one used in RMAN99, the latter being closer to the recent determinations (e.g., Jacobson and Lainey 2014). By rescaling BS99 series with the H_D value and Phobos mass of RMAN99, the differences in the time domain between the two series are reduced to 1 mas in longitude and 0.1 mas in obliquity (see panels c and d of Fig. 2), and up to 0.4 mas term by term, still 4 times larger than the truncation criterion. Note that by rescaling the RK79 time series with the H_D of RMAN99, the differences between the RK79 series and the RMAN99 or the rescaled BS99 series can reach up to 4 mas (see Table 1), ten times the differences between the RMAN99 and rescaled BS99 series. It mainly results from the fact that the RK79 series concern the axis of figure of Mars, whereas the other series are for the angular momentum axis of Mars (see Sect. 3.7).

It is necessary to elucidate the origin of the remaining differences between the RMAN99 and the rescaled BS99 series in order to avoid introducing bias in the interpretation of future radioscience data in terms of interior structure. To that end, we recompute the RMAN99

that is to say as if Mars was evolving on an osculating orbit. The factor $P_2^0(\sin\delta)$ is expressed as a function of spherical coordinates which are converted from the rectangular coordinates of Mars in the VSOP87.

[4] And therefore implicitly for *all* the secular variations of the mean orbital elements, not just for the secular variations in eccentricity or inclination.

[5] Under the "Keplerian assumption," the modulations in nutation amplitude can be obtained by extracting the long-period arguments (the orbital elements other than the mean anomaly, see Sect. 3.4.2) from the sine and cosine developments through a linearization around their epoch values.

[6] The solution is obtained after repeated trigonometric manipulations of a large amount of terms. When the computation speed and random-access memory are too limited, as was the case 20 years ago, approximations which alter the accuracy of the solution must be done during the computation. See details of the computation procedure of the recomputed RMAN99 solution in Sect. 4.

[7] The value 0.00536 reported in RMAN99 is in fact a wrong rounding of the value actually used, Fabian Roosbeek, personal communication.

Table 1 Amplitudes[a] (in mas) of the main terms of the nutation series of RK79[c], BS99[b], and RMAN99[d] in longitude ($\Delta\psi$) and in obliquity ($\Delta\varepsilon$), as defined in Eq. (15)

	RK79		RK79 rescaled		BS99		BS99 rescaled		RMAN99		RMAN99 recomputed	
H_D	0.005346		0.00535464		0.005363		0.00535464		0.00535464		0.00535464	
$\mathcal{M}_{Ph}$	–		–		1.28×10^{16} kg		1.05×10^{16} kg		1.05×10^{16} kg		1.05×10^{16} kg	
Arg.	cos	sin	cos	sin	cos	sin	cos	sin	cos	sin	cos	sin
$(\Delta\psi)$												
$1Ma$	−282.06	−476.81	−282.52	−477.58	−282.92	−478.51	−282.47	−477.76	−282.42	−477.62	−282.48	−477.76
$2Ma$	−221.21	−1110.34	−221.56	−1112.14	−221.22	−1110.32	−220.87	−1108.59	−220.64	−1108.21	−220.92	−1108.48
$3Ma$	−137.47	−200.70	−137.69	−201.02	−137.29	−200.39	−137.08	−200.08	−137.00	−200.03	−137.08	−200.06
$4Ma$	−34.60	−21.81	−34.65	−21.85	−34.89	−21.70	−34.83	−21.66	−34.82	−21.66	−34.83	−21.66
$5Ma$	−6.43	−0.94	−6.44	−0.94	−6.23	−0.91	−6.22	−0.91	−6.26	−0.89	−6.26	−0.88
$6Ma$	−0.96	0.27	−0.96	0.27	−0.90	0.25	−0.89	0.25	−0.89	0.25	−0.89	0.25
$7Ma$	–	–	–	–	−0.10	0.08	−0.10	0.08	−0.10	0.00	−0.10	0.08
$-N_{Ph}$	–	–	–	–	0	12.09	0.00	9.88	0.00	9.88	0.00	9.88
$-N_{De}$	–	–	–	–	0	4.39	0.00	4.38	0.00	4.39	0.00	4.39
$(\Delta\varepsilon)$												
$1Ma$	47.27	12.08	47.34	12.10	47.74	11.95	47.66	11.93	47.68	11.94	47.67	11.91
$2Ma$	−508.04	88.58	−508.86	88.72	−508.23	88.58	−507.44	88.44	−507.4	88.41	−507.46	88.48
$3Ma$	−93.70	62.80	−93.85	62.90	−93.66	62.76	−93.51	62.66	−93.51	62.65	−93.51	62.67

Table 1 continued

	RK79		RK79 rescaled		BS99		BS99 rescaled		RMAN99		RMAN99 recomputed	
H_D	0.005346		0.00535464		0.005363		0.00535464		0.00535464		0.00535464	
$\mathcal{M}_{Ph}$	–		–		1.28×10^{16} kg		1.05×10^{16} kg		1.05×10^{16} kg		1.05×10^{16} kg	
Arg.	cos	sin	cos	sin	cos	sin	cos	sin	cos	sin	cos	sin
$4Ma$	−10.24	16.24	−10.26	16.27	−10.22	16.22	−10.21	16.19	−10.21	16.19	−10.21	16.19
$5Ma$	−0.43	2.97	−0.43	2.97	−0.43	2.93	−0.43	2.92	−0.43	2.93	−0.43	2.93
$6Ma$	0.11	0.39	0.11	0.39	0.12	0.42	0.12	0.42	0.12	0.42	0.12	0.42
$-N_{Ph}$	–	–	–	–	−5.14	0.00	−4.20	0.00	−4.20	0.00	−4.20	0.00
$-N_{De}$	–	–	–	–	−1.87	0.00	−1.87	0.00	−1.86	0.00	−1.86	0.00

RK79 series include 6 solar terms. BS99 and RMAN99 series include 7/6 solar terms in longitude/obliquity, as well as one Phobos and one Deimos terms. Following RMAN99, we express the solar terms as functions of harmonics of the VSOP87 argument $Ma = 355°.4329996 + 689050774''.940\,t$, the mean longitude of Mars with t the time measured in thousand of years from J2000. The Phobos/Deimos terms correspond to the arguments $N_{Ph} = 125°.8759 - 159257°.97707018\,T$ and $N_{De} = 11°.1971 - 6574°.96623684\,T$, with T the time measured in thousands of Julian years from J2000, representing the satellites' orbital nodes taken from ESAPHO and ESADE (see Eq. 21 of RMAN99). Alternative forms of the RK79 and BS99 series are rescaled for the value of the H_D factor and the mass of Phobos $\mathcal{M}_{Ph}$. An alternative form of RMAN99, given in the last column, corresponds to a recomputation using modern computer capabilities (see Sect. 4.1). The best agreement is obtained between the recomputed RMAN99 series and the rescaled BS99 series (differences ≤ 0.1 mas term by term)

[a]Here, we consider prograde angles and ascending nodes of moving planes with respect to fixed planes. As a result, if we have a + sign for a given term of the series for the nutation in longitude, the signs for the corresponding terms in the original series of RK79, RMAN99, and BS99 are +, +, and −, respectively. If we have a + sign for a given term of the series for the nutation in obliquity, the signs for the corresponding terms in the original series of RK79, RMAN99, and BS99 are +, −, and +, respectively

[b]The solar terms of BS99 series are originally expressed as functions of the arguments $M_M = M_0 + nt$, the mean anomaly of Mars with $n \cong \dot{Ma}$, and Λ, the orbital perigee of Mars measured from the node between Mars orbit and Mars equator. To express BS99 series as a function of Ma, we consider that $n = \dot{Ma}$ and $M_0 = (Ma - \varpi)|_{t=0} = 19°.37276563$, with ϖ the pericenter longitude as given by Simon et al. (1994) for the mean orbital elements of Mars consistent with VSOP87. We also considered that $\Lambda = (\varpi - \Omega - \theta_M)|_{t=0} = 251°.005323169$ with Ω the orbital node of Mars with respect to the J2000 ecliptic and θ_M the angle between the orbital node with respect to the ecliptic and the node between Mars orbit and Mars equator (see Eq. 3 of RMAN99 for the numerical values). We find that the use of those values ensures the best agreement between RMAN99 and BS99 series. For instance, using the JPL *Keplerian Elements for Approximate Positions of the Major Planets* (https://ssd.jpl.nasa.gov/?planet_pos), and therefore, $M_0 = 19°.3902$ ($+0°.02$ with respect to the value consistent with VSOP87) would introduce differences up to the mas level in the time domain due to an artificial dephasing between the BS99 and the RMAN99 series

[c]For the sake of comparison, we also re-express RK79 series as function of Ma only, using the same values for M_0 and Λ as for re-expressing the BS99 series. Note that RK79 introduce the argument $q = 2\Lambda$, so we use $q = 142°.010646338$, instead of $q = 142°.0$ as done, e.g., in Konopliv et al. (2006)

[d]Note that the column headers sin and cos in Tables 2 and 3 of RMAN99 are reversed

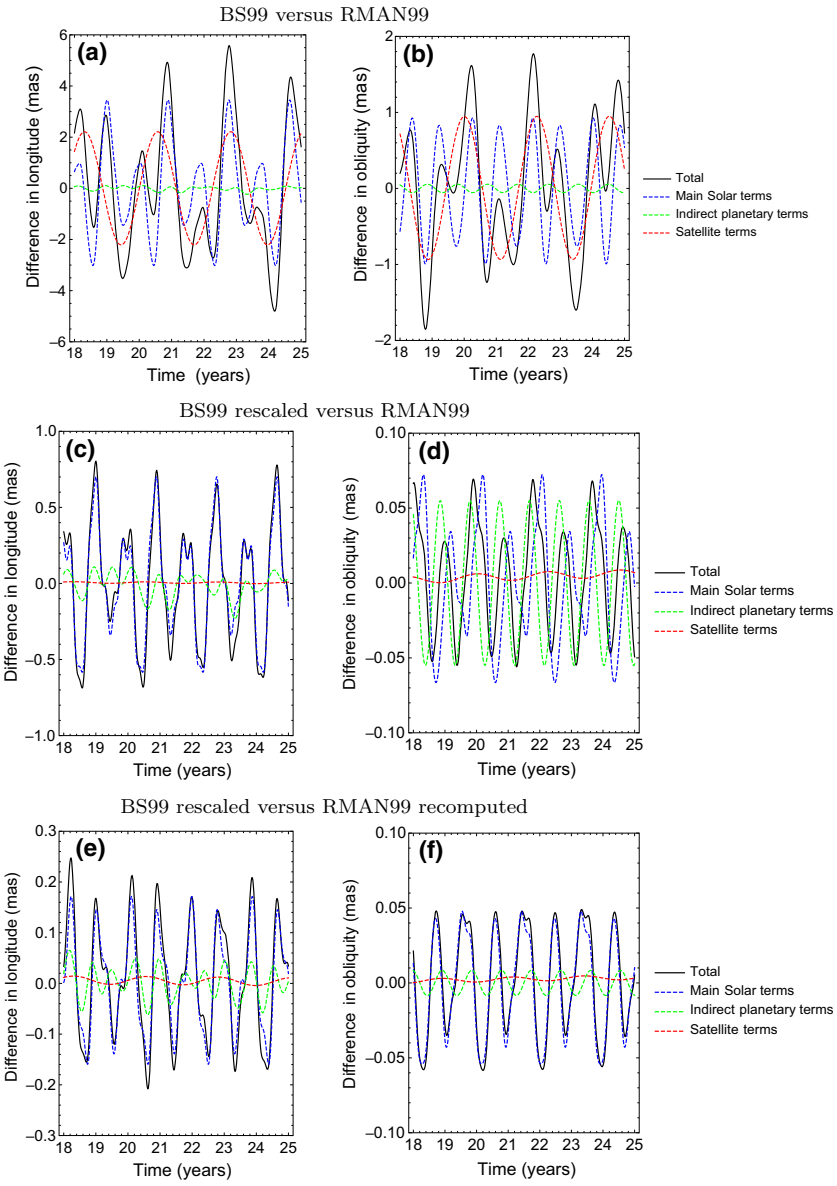

Fig. 2 Black curves: differences, as a function of time, between the nutations in longitude (left) and in obliquity (right) computed from the series of BS99 (considering the main solar terms, the indirect planetary terms, and the satellite terms, but not the mixed and direct planetary terms, which have no counterparts in RMAN99) and the nutations computed from the series of RMAN99. Very long period terms are not included in the comparison, since the computational procedure of RMAN99 can make them artificially large or small (and so wrongly included or not in the final series), see Sect. 4.1.3. Blue, green, and red curves are for the differences between the main solar terms, the indirect planetary terms, and the satellite terms, respectively. The time is measured in years past J2000. The differences in solar terms are mainly related to the annual and semi-annual terms (see also Table 1). The differences in satellites terms is mainly related to Phobos. Top panels: differences between BS99 and RMAN99 original series. Middle panels: as in top panels, except that BS99 series are rescaled to the scaling factor H_D and Phobos mass used in RMAN99. Bottom panels: as in middle panels, except that RMAN99 series are recomputed using modern computer capabilities (see Sect. 4.1)

series, using the same ephemerides (VSOP87, ESAPHO, ESADE) as for the original series, but taking advantage of modern computer performances. The assumptions made at the time are also examined (see details in Sect. 4.1). We will show that the so obtained recomputed series is in a better agreement with the rescaled BS99 series ($\lesssim 0.1$ mas term by term, the difference being relatively smaller for the dominant terms: 0.01% on the semi-annual term but 0.6% for the fifth term, for instance). The difference is at most 0.01% in the time domain (see panels e and f of Fig. 2) and on the first three dominating terms, and can be seen as modeling uncertainties resulting from the different physical assumptions considered in the two approaches.

Compared to the expected precision on future nutation measurements (a few mas), the choice between the two approaches (Hamiltonian versus Torque approach) can be seen as a matter of convenience. The VSOP87 is about 30 years old and itself adjusted to numerical ephemerides (DE200, Standish 1982) 6 years older. Using the Torque approach, we thus determine an updated rigid nutation series (BMAN20), using the more recent ephemerides VSOP2000 which has the advantage of being expressed in a similar format as VSOP87 (Moisson and Bretagnon 2001), see Sects. 4.2 and 4.3. In these sections, we also show that the variations of the rigid nutation amplitudes that would be induced by the use of other recent ephemerides (e.g., the numerical ephemerides DE431) would be small compared to the difference between the recomputed RMAN99 and the updated BMAN20 series.

3 Governing equations and analytical solutions

The variations in the rotation of Mars can be separated into the variations in rotation speed around its spin axis (length-of-day variations, ΔLOD) and the variations in orientation of the spin axis in space (precession/nutation) and with respect to the surface of the planet (polar motion). In this section, we aim to set the theoretical grounds for the study of the precession and nutations. As the differential motion between the angular momentum (AM) and spin axes is negligible (BS99, RMAN99), we derive the governing equations for the precession/nutation of the angular momentum (AM) axis of Mars in space. We follow the Torque approach, starting from the definition of the Euler angles of the figure axis, since the rotation of Mars can simply be described by the temporal evolution of the Euler angles from an Inertial Frame (IF) to the rotating Body Frame (BF) of Mars. We make the connection between the governing equations of RK79 for the motion of the figure axis and of RMAN99 for the motion of the angular momentum axis.

3.1 The Euler angles and the rotation matrix

The Euler angles for the figure axis are the node longitude ψ, the obliquity ε, and the rotation angle ϕ (see Fig. 3). We consider prograde angles and ascending nodes of moving planes with respect to fixed planes. The IF is centered at the center of mass of Mars and chosen to be associated with the mean orbital plane of Mars at a reference epoch (J1978.0 in RK79,[8]

[8] As RK79 do not impose the epoch values of their arguments M and q, it is possible to consider values referred to the mean orbit of Mars at epoch J2000 when using their series, as, e.g., in Konopliv et al. (2016) and in Table 1.

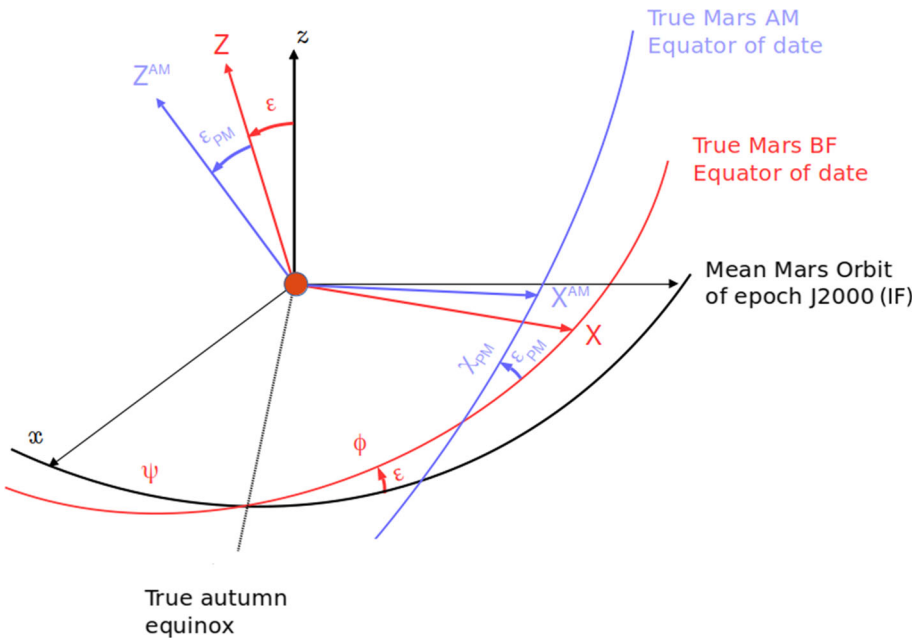

Fig. 3 Euler angles (defined as prograde angles) between the rotating BF of Mars (axes XYZ, in red) and the IF associated with the mean orbit of Mars at epoch J2000 (axes xyz in black, the x-axis is in the direction of the ascending node of Mars orbit over the Earth ecliptic of epoch J2000). The X-axis of the BF is chosen as the prime meridian defined in the IAU convention (Archinal et al. 2018). ψ is measured from the x-axis to the autumn equinox, ϕ is measured from the equinox to the X-axis, and ε is the angle from the z-axis to the Z-axis, or the inclination of the BF equator over the IF xy plane. The term "true autumn equinox" is here an abuse of terminology, as the true Autumn equinox is in principle the ascending node of the true equator over the true orbit of date. The angular momentum axis does not coincide with the figure axis of Mars. They are inclined by ε_{PM} to each other, and χ_{PM} is measured from the node of the AM equator over the BF equator to the X^{AM}-axis (the subscript PM stands for *Polar Motion*, the differential motion between the figure and spin axes. We here consider that the AM and spin axes are aligned to each other, see BS99 and RMAN99). Beware that throughout the text, the notations ψ, ε, and ϕ are also used for the Euler angles of the AM axis

J2000 in RMAN99,[9] BS99,[10] and in this paper). The BF is attached to the principal axes of inertia of the planet, its X and Y axes define the equator of figure of Mars, and its Z axis defines the figure axis.

The rotation matrix from the BF to the IF can be expressed in terms of the **figure axis Euler angles** $(\psi, \varepsilon, \phi)$ as

$$\mathbf{M} = \mathbf{R_z}(-\psi) \cdot \mathbf{R_x}(-\varepsilon) \cdot \mathbf{R_z}(-\phi). \tag{1}$$

[9] Contrary to what is stated in RMAN99, his nutation series are referred to the mean orbit and equinox of epoch J2000 and not of date, as he sets $t = 0$ in his Eq. (3) (Roosbeek, personal communication).

[10] The nutation series of BS99 are in fact referred to the non-inertial mean orbital plane of date. They introduce a complementary term in their Hamiltonian to account for the motion of the reference frame with respect to the mean orbital plane of epoch J2000, which results in complementary secular variations of the longitude and obliquity of Mars BF (see their Sect. 5). Neglecting those complementary variations therefore approximately amounts to consider the mean orbital plane of epoch J2000 as the reference plane, so that comparison between the different nutation theories is possible, and done in Table 1 and Fig. 2.

Alternatively, the transformation can be expressed as (Folkner et al. 1997a; Konopliv et al. 2006; Le Maistre et al. 2012)

$$\mathbf{M} = \mathbf{R_z}(-\psi) \cdot \mathbf{R_x}(-\varepsilon) \cdot \mathbf{R_z}(-\phi) \cdot \mathbf{R_y}(X_P) \cdot \mathbf{R_x}(Y_P), \tag{2}$$

where $(\psi, \varepsilon, \phi)$ are the **AM axis Euler angles**. The projection of the unit vector along the AM axis in the BF is often denoted $(X_P, -Y_P)$ with the minus sign in front of Y_P coming from the convention used for Earth polar motion, but can also be expressed as $(-\varepsilon_{PM} \sin \chi_{PM}, -\varepsilon_{PM} \cos \chi_{PM})$, with χ_{PM} and ε_{PM}, the angles from the BF to the AM frame (see Fig. 3).

The advantage of the rotation matrix of Eq. (1), as used in RK79, is that it avoids the need to introduce polar motion terms. The rotation matrix of Eq. (2) is more convenient for interpreting Doppler data in terms of nutations and polar motion separately. Nutations are usually associated with external gravitational torques and modeled in the IF, whereas polar motion is usually associated with surface torques due to AM exchanges with the atmosphere and modeled independently in the rotating BF. It should be kept in mind that it is not consistent to introduce the nutations series of RK79 for the figure axis into a rotation matrix such as that of Eq. (2). Yet, that is what is done in, e.g., Folkner et al. (1997b), Konopliv et al. (2006, 2016) and Kuchynka et al. (2014). Such practice could lead to a significant bias in the interpretation of future nutation measurements in terms of the core characteristics, as the difference of the order of the mas between the AM and figure axes (Oppolzer terms, see Sect. 3.7) could be wrongly interpreted as part of the amplification related to the fluid core. It is more appropriate to introduce an AM nutations series, as done recently in Folkner et al. (2018) and Dehant et al. (2020).

3.2 Angular momentum equation

In the rotating BF, the angular momentum equation can be written as

$$\frac{\partial \mathbf{H}}{\partial t} + \boldsymbol{\Omega} \wedge \mathbf{H} = \boldsymbol{\Gamma}. \tag{3}$$

Here, $\boldsymbol{\Omega}$ is the angular velocity vector of rotation (or rotation vector, see Eq. 5a), $\boldsymbol{\Gamma} = (\Gamma_X, \Gamma_Y, \Gamma_Z)$ is the total torque exerted on the planet, and $\mathbf{H} = \mathbb{I}\,\boldsymbol{\Omega}$ is the angular momentum, with the inertia tensor

$$\mathbb{I} = \begin{pmatrix} A & 0 & 0 \\ 0 & B & 0 \\ 0 & 0 & C \end{pmatrix}. \tag{4}$$

The components of the rotation vector are customarily written as

$$\boldsymbol{\Omega} = \begin{pmatrix} \omega_1 \\ \omega_2 \\ \omega_3 \end{pmatrix} = \Omega_R \begin{pmatrix} m_1 \\ m_2 \\ 1 + m_3 \end{pmatrix}, \tag{5a}$$

with Ω_R the mean rotation rate. The variation rates $\dot{\psi}$, $\dot{\varepsilon}$, and $\dot{\phi}$ of the Euler angles of the figure axis describe successive rotations of the planet about the z-axis, the autumn equinox axis, and the Z-axis, respectively, so that, as observed from the BF, the rotation vector writes (e.g., Dehant and Mathews 2015):

$$\mathbf{\Omega} = \mathbf{R_z}(\phi)\cdot\mathbf{R_x}(\varepsilon)\cdot\begin{pmatrix}0\\0\\\dot{\psi}\end{pmatrix} + \mathbf{R_z}(\phi)\cdot\begin{pmatrix}\dot{\varepsilon}\\0\\0\end{pmatrix} + \begin{pmatrix}0\\0\\\dot{\phi}\end{pmatrix},$$
$$= \begin{pmatrix}\dot{\psi}\sin\varepsilon\sin\phi + \dot{\varepsilon}\cos\phi\\ \dot{\psi}\sin\varepsilon\cos\phi - \dot{\varepsilon}\sin\phi\\ \dot{\phi} + \cos\varepsilon\,\dot{\psi}\end{pmatrix}. \tag{5b}$$

We include the gravitational torques by the Sun, Phobos, Deimos, and the planets. Here, we neglect the torque produced by the atmosphere dynamics of Mars, as it can be shown that its effect on the precession/nutation is negligible (see Sect. 3.7). We also consider the "rigid nutations" in the sense of no fluid layer/atmosphere dynamics. We momentarily assume that the planet is axisymmetric ($A = B = \bar{A}$, with $\bar{A} = (A+B)/2$ the mean equatorial moment of inertia), in order to retrieve the equations of RK79. We will introduce the effect of triaxiality subsequently. We also assume that $\Gamma_Z = 0$, as we do not study the variations in LOD. At first order in small quantities (ω_1 and ω_2), the three components of the angular momentum equation (3) can then be written as

$$\bar{A}\dot{\omega}_1 + (C-\bar{A})\omega_3\omega_2 = \Gamma_X, \tag{6a}$$
$$\bar{A}\dot{\omega}_2 + (\bar{A}-C)\omega_3\omega_1 = \Gamma_Y, \tag{6b}$$
$$C\dot{\omega}_3 = 0. \tag{6c}$$

Equation (6c) indicates that ω_3 is a constant, which is the mean rotation rate of the planet Ω_R. Note that the quantities X_P and Y_P introduced in Eq. (2) are equal to m_1 and $-m_2$, respectively. After substitution of Eq. (5b), Eqs. (6a, 6b) can be written as

$$\bar{A}\ddot{\varepsilon} + \dot{\psi}\sin\varepsilon(C\Omega_R - \bar{A}\dot{\psi}\cos\varepsilon) = \Gamma_X\cos\phi - \Gamma_Y\sin\phi, \tag{7a}$$
$$\bar{A}\ddot{\psi}\sin\varepsilon - \dot{\varepsilon}(C\Omega_R - 2\bar{A}\dot{\psi}\cos\varepsilon) = \Gamma_X\sin\phi + \Gamma_Y\cos\phi, \tag{7b}$$

which are second-order differential equations equivalent to Eqs. (5–6) of RK79 derived from the Lagrangian of the system that govern the nutations of the figure axis (Z-axis of the BF). As explained by RK79, after Woolard (1953), by neglecting the square and products of $\dot{\psi}$ and $\dot{\varepsilon}$ and the second derivative terms $\ddot{\psi}$ and $\ddot{\varepsilon}$, and by taking $\sin\varepsilon_0$ instead of $\sin\varepsilon$ in front of $\dot{\psi}$ in Eqs. (7a, 7b), one obtains equations governing the nutations of the AM axis. In the triaxial case ($A \neq B$), we have, after similar manipulations as in the axisymmetric case,

$$\dot{\psi}\sin\varepsilon_0\,\Omega_R = \frac{\Gamma_X}{C+A-B}\cos\phi - \frac{\Gamma_Y}{C+B-A}\sin\phi, \tag{8a}$$
$$-\dot{\varepsilon}\,\Omega_R = \frac{\Gamma_X}{C+A-B}\sin\phi + \frac{\Gamma_Y}{C+B-A}\cos\phi. \tag{8b}$$

The torque, in the coordinates of the rotating BF, can be written as (e.g., Murray and Dermott 1999)

$$\mathbf{\Gamma} = 3\frac{GM_B}{d_B^5}\begin{pmatrix}(C-B)\tilde{Y}_B\tilde{Z}_B\\ (A-C)\tilde{X}_B\tilde{Z}_B\\ 0\end{pmatrix}, \tag{9}$$

with $\tilde{\mathbf{r}}_\mathbf{B} = (\tilde{X}_B, \tilde{Y}_B, \tilde{Z}_B)$ the position of the perturbating body, d_B its distance to the center of Mars, M_B its mass, and G the gravitational constant. We transform the $(\tilde{X}_B, \tilde{Y}_B, \tilde{Z}_B)$ coordinates according to

$$\tilde{\mathbf{r}}_{\mathbf{B}} = \mathbf{R}_{\mathbf{z}}(\phi) \cdot \mathbf{r}_{\mathbf{B}} = \begin{pmatrix} \cos\phi\, X_B + \sin\phi\, Y_B \\ -\sin\phi\, X_B + \cos\phi\, Y_B \\ \tilde{Z}_b \end{pmatrix}, \tag{10}$$

with $\mathbf{r_B} = (X_B, Y_B, Z_B)$ the position in the coordinates of an alternative BF whose x-axis is in the direction of the autumn equinox. This *equinox BF* precesses and nutates as the true BF of date precesses and nutates with respect to the mean orbit of the chosen epoch.

Correct up to the first order in the differences $(A - \bar{A})$ and $(B - \bar{A})$, Eqs. (8a, 8b) are now written as

$$\dot{\psi} = \frac{3H_D G M_B}{\sin\varepsilon_0 \Omega_R} \frac{Y_B Z_B}{d_B^5} + \frac{3\,\delta H_D^{\rm tri} G M_B}{2\sin\varepsilon_0 \Omega_R} \frac{X_B Z_B \sin 2\phi - Y_B Z_B \cos 2\phi}{d_B^5}, \tag{11a}$$

$$\dot{\varepsilon} = \frac{3H_D G M_B}{\Omega_R} \frac{X_B Z_B}{d_B^5} + \frac{3\,\delta H_D^{\rm tri} G M_B}{2\Omega_R} \frac{X_B Z_B \cos 2\phi + Y_B Z_B \sin 2\phi}{d_B^5}, \tag{11b}$$

with

$$H_D = (C - \bar{A})/C, \tag{11c}$$

$$\delta H_D^{\rm tri} = (B - A)/C. \tag{11d}$$

H_D is the *dynamical flattening* of Mars, also called *scaling factor*, as the nutation series can always be rescaled to a chosen value of H_D, as we did in Table 1.

Equations (11a, 11b) are first-order linear differential equations in $\dot{\psi}$ and $\dot{\varepsilon}$. As Mars' rotation is faster than its revolution, the response to the external torques is divided into two distinct parts. The first part does not depend on the variations of the rotation angle ϕ and on the triaxiality.[11] If $\delta H_D^{\rm tri}$ is neglected [or Eqs. (11a, 11b) are averaged over the rotation angle ϕ], the AM equations become

$$\dot{\psi} = \frac{3H_D G M_B}{\sin\varepsilon_0 \Omega_R} \frac{Y_B Z_B}{d_B^5}, \tag{12a}$$

$$\dot{\varepsilon} = \frac{3H_D G M_B}{\Omega_R} \frac{X_B Z_B}{d_B^5}, \tag{12b}$$

and are equivalent to the governing equations (15–16) of RMAN99 and Eq. (4) of Hilton (1991), which are easier to integrate than Eqs. (7a, 7b) and Eqs. (5–6) of RK79.

The part of the AM equations proportional to $\delta H_D^{\rm tri}$ is related to the triaxiality and induces quasi semi-diurnal nutations of small amplitudes, since ϕ is a fast angle. In the BMAN20 solution, we will find only one term above our truncation criterion, with an amplitude in longitude of the order of 0.1 mas (see also RK79, BS99, and Borderies 1980).

H_D and $\delta H_D^{\rm tri}$ are related to the second-degree gravity field coefficients (see Eqs. 11c, 11d, 77). We neglected the effect of high-order gravity coefficients (e.g., J_3) on the precession/nutation. The effect of J_3 on the amplitude of the annual nutation is about 0.0006 mas, as can be verified from the integration of Eqs. (56–57) of Roosbeek and Dehant (1998).

[11] To the best of our knowledge, Groten et al. (1996) are the only one to find an effect of the triaxiality on the scaling factor H_D, and therefore on the precession rate and the main nutation terms. However, it has been shown that triaxiality does not change the main precession/nutation behavior of Mars (e.g., Newman 2013), but induces only small semi-diurnal nutations (e.g., BS99), as we find in this paper.

3.3 Different precession/nutation representations

The orientation of the spin axis is usually described by two angles: the node longitude and the obliquity with respect to the orbital plane, whose periodic variations can be expressed with periodic series. Alternatively, the wiggly trajectory of the spin axis in space can also be expressed as series of prograde and retrograde circular motions, or as variations in right ascension and declination with respect to the ICRF J2000, as in the IAU conventions.

3.3.1 Longitude/obliquity representation

Usually (e.g., RK79, RMAN99, BS99), the solution for the Euler angles ψ and ε of the AM or figure axis is expressed in the form of

$$\psi = \psi_0 + \dot{\Psi}\, t + \Delta\psi, \tag{13a}$$

$$\varepsilon = \varepsilon_0 + \dot{E}\, t + \Delta\varepsilon. \tag{13b}$$

The angles ψ_0 and ε_0 are integration constants for ψ and ε, respectively, which can be obtained from the observed spin orientation at the reference epoch. Some authors do not include the longitude integration constant in the solution (e.g., RK79). Apart from the integration constant, ψ is decomposed into a slow uniform precession around the z-axis at rate $\dot{\Psi}$ and periodic nutations in longitude $\Delta\psi$. The obliquity is the sum of ε_0, of a very slow secular variation (see BS99), and of periodic nutations $\Delta\varepsilon$. The BMAN20 solution (Sect. 4.3) includes quadratic terms:

$$\psi = \psi_0 + \dot{\Psi}\, t + \frac{\ddot{\Psi}}{2}\, t^2 + \Delta\psi, \tag{14a}$$

$$\varepsilon = \varepsilon_0 + \dot{E}\, t + \frac{\ddot{E}}{2}\, t^2 + \Delta\varepsilon. \tag{14b}$$

We introduced the notation $\dot{\Psi}$ and $\dot{E}$ for the secular variation rates, to avoid confusion with $\dot{\psi}$ and $\dot{\varepsilon}$, the time derivatives of ψ and ε, as used in Eqs. (12a, 12b).

In the following, as in RMAN99, the nutations series in longitude and in obliquity will be written as

$$\left\{ \begin{array}{c} \Delta\psi \\ \Delta\varepsilon \end{array} \right\} = \sum_j \left(\left\{ \begin{array}{c} \psi_j^c \\ \varepsilon_j^c \end{array} \right\} \cos\varphi_j + \left\{ \begin{array}{c} \psi_j^s \\ \varepsilon_j^s \end{array} \right\} \sin\varphi_j \right), \tag{15}$$

with $\psi/\varepsilon_j^{c/s}$ the amplitudes and $\varphi_j = f_j t + \varphi_j^0$ a linear combination of fundamental arguments (here, the mean longitude of Mars, the Earth, Venus, Jupiter, and Saturn, and the nodes of Phobos and Deimos). In RMAN99, the nutation amplitudes are constant with time. In BS99 and in BMAN20 solutions (Sect. 4.3), the nutation amplitudes change with time.

For later use, we define the mean node longitude and obliquity (using the notations θ_M and ε_M of Eq. (3) of RMAN99):

$$\theta_M = \psi_0 + \dot{\Psi}\, t = \theta_0 + \dot{\theta}\, t, \tag{16a}$$

$$\varepsilon_M = \varepsilon_0 + \dot{E}\, t. \tag{16b}$$

In this paper, as in RMAN99, the notations ψ and ε are preferably used for the output of the computation (the solution), whereas the notations θ_M and ε_M are used for the input (the torque computation). We now return to the definition of the *equinox BF* given earlier after Eqs. (9, 10) for the torque. The x-axis of the equinox BF lies in the xy plane of the IF

(the mean Mars orbit of epoch J2000), at the angular distance ψ from the x-axis of the IF. Similarly, the angles θ_M and θ_0 define the x-axes of the *mean equinox BF of date* and of the *J2000 mean equinox BF*, respectively. The mean (equinox) BF is defined so that it follows the precession but not the nutations.

3.3.2 Prograde/retrograde representation

The nutations of the angles ψ and ε for the AM axis (or figure axis) are often related to the corresponding periodic variations in the projection of the trajectory of a unit vector along the AM (figure) axis onto the equator of the J2000 mean equinox BF (Defraigne et al. 1995), denoted $(\delta x, \delta y)$. Omitting the linear and quadratic terms in Eqs. (14a, 14b), the components of the unit vector along the figure axis (AM axis) in the J2000 mean equinox BF are given around J2000, at first order in small variations, by

$$\begin{pmatrix} \delta x \\ \delta y \\ 1 \end{pmatrix} = \mathbf{R_x}(\varepsilon_0) \cdot \mathbf{R_z}(\psi_0 - \psi) \cdot \mathbf{R_x}(-\varepsilon) \cdot \begin{pmatrix} 0 \\ 0 \\ 1 \end{pmatrix} = \begin{pmatrix} \sin\varepsilon_0 \Delta\psi \\ -\Delta\varepsilon \\ 1 \end{pmatrix}. \tag{17}$$

The projection can be expressed as series of prograde and retrograde circular motions

$$\begin{Bmatrix} \delta x \\ \delta y \end{Bmatrix} = \sum_j \left(\mathcal{P}_j \begin{Bmatrix} \cos \\ \sin \end{Bmatrix} (f_j t + \pi_j) + \mathcal{R}_j \begin{Bmatrix} \cos \\ \sin \end{Bmatrix} (-f_j t - \rho_j) \right), \tag{18}$$

with amplitudes $\mathcal{P}_j$ and $\mathcal{R}_j$ and phases π_j and ρ_j at J2000 that are related to those of the series for the longitude and obliquity nutations by:

$$\mathcal{P}_j = \sqrt{\left(\frac{\sin\varepsilon_0\, \psi_j^c - \varepsilon_j^s}{2} \right)^2 + \left(\frac{\sin\varepsilon_0\, \psi_j^s + \varepsilon_j^c}{2} \right)^2}, \tag{19a}$$

$$\mathcal{R}_j = \sqrt{\left(\frac{\sin\varepsilon_0\, \psi_j^c + \varepsilon_j^s}{2} \right)^2 + \left(\frac{\sin\varepsilon_0\, \psi_j^s - \varepsilon_j^c}{2} \right)^2}, \tag{19b}$$

$$\cos(\pi_j - \varphi_j^0) = \frac{\sin\varepsilon_0\, \psi_j^c - \varepsilon_j^s}{2\mathcal{P}_j}, \tag{19c}$$

$$\sin(\pi_j - \varphi_j^0) = \frac{-\sin\varepsilon_0\, \psi_j^s - \varepsilon_j^c}{2\mathcal{P}_j}, \tag{19d}$$

$$\cos(\rho_j - \varphi_j^0) = \frac{\sin\varepsilon_0\, \psi_j^c + \varepsilon_j^s}{2\mathcal{R}_j}, \tag{19e}$$

$$\sin(\rho_j - \varphi_j^0) = \frac{-\sin\varepsilon_0\, \psi_j^s + \varepsilon_j^c}{2\mathcal{R}_j}. \tag{19f}$$

3.3.3 Right ascension and declination

The angles ψ and ε for the AM axis (figure axis) can also be related to (α, δ), the equatorial coordinates of a unit vector along the AM axis (figure axis) in the ICRF (see, e.g., Fig. 1 of

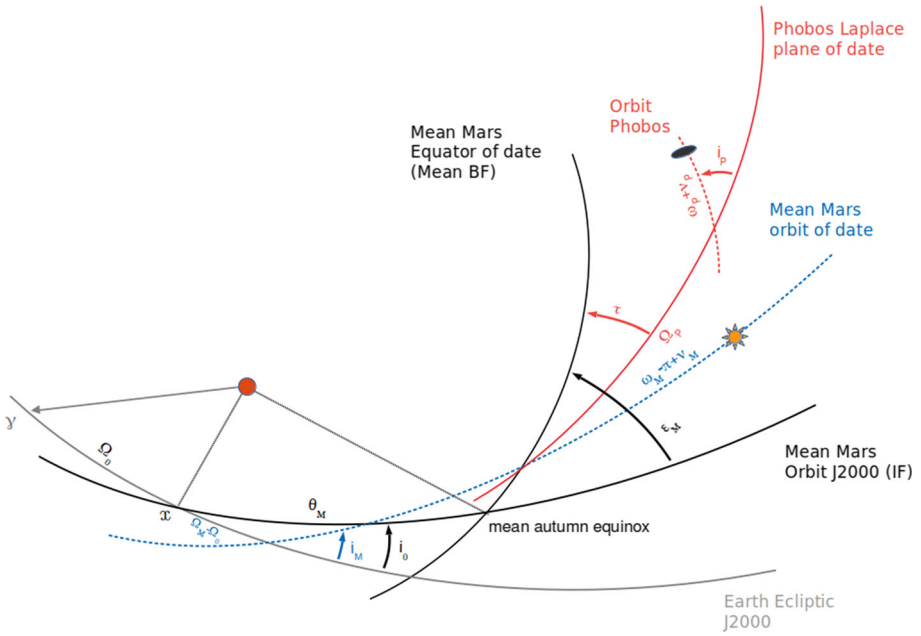

Fig. 4 Angles defining the positions of the Sun and of Phobos for the simple case of precessing Mars (the Sun orbit, as seen from Mars) and Phobos orbits. The angles $(\Omega_0, i_0) = (\Omega_M, i_M)|_{t=0}$ and $(\theta_M, \varepsilon_M)$ allow the transformation from the ecliptic reference frame to the mean equinox BF of date [see Fig. 1 of RMAN99 and Eq. (16a)]. The origin γ of the ecliptic is the ascending node on the J2000 Earth equator. Ω_P and i_P are the ascending node and inclination, respectively, of the orbit of Phobos with respect to the local Laplace plane. ω_M and ω_P are the arguments of the pericenters of the orbit of Mars and of Phobos, respectively. $\omega_M - \pi - \theta_M$ is the longitude of the pericenter of the Sun with respect to the mean autumn equinox for a non-precessing orbit (see argument $q = 2(\omega - \theta)$ in RK79). τ is the tilt between Mars equator and the local Laplace plane of Phobos. The Laplace plane and the equator share their node on the mean orbit. ν_M and ν_P are the true anomalies. Numerical values for the angles are given in Table 2

Archinal et al. 2018). The coordinates of the unit vector along the AM axis (figure axis) in the coordinate system of the IF are given by

$$\begin{pmatrix} X_f \\ Y_f \\ Z_f \end{pmatrix} = \mathbf{R_x}(i_0) \cdot \mathbf{R_z}(\Omega_0) \cdot \mathbf{R_x}(\varepsilon_{\text{Earth}}) \cdot \begin{pmatrix} \cos\delta\cos\alpha \\ \cos\delta\sin\alpha \\ \sin\delta \end{pmatrix}, \tag{20}$$

with i_0 and Ω_0 the mean orbital inclination and node longitude of Mars (see Fig. 4). The angles (ψ, ε) can then be related to (α, δ) by using the trigonometric relations

$$\varepsilon = \arccos Z_f, \tag{21a}$$

$$\psi = \frac{\pi}{2} + \arctan\frac{Y_f}{X_f}. \tag{21b}$$

There, $\psi_0 = \theta_0 \simeq 35°$, measured from the intersection of the mean Mars orbit of epoch on the ecliptic of epoch (see Fig. 4), as in, e.g., Folkner et al. (1997b).

Alternatively, (X_f, Y_f, Z_f) can also be defined as

$$\begin{pmatrix} X_f \\ Y_f \\ Z_f \end{pmatrix} = \mathbf{R_x}(J) \cdot \mathbf{R_z}(N) \cdot \begin{pmatrix} \cos\delta\cos\alpha \\ \cos\delta\sin\alpha \\ \sin\delta \end{pmatrix}, \tag{22}$$

with J and N the inclination and node longitude of the mean Mars orbit of epoch with respect to the ICRF equator. In that case, $\psi_0 = \theta_0 \simeq 82°$ is measured from the intersection of the mean Mars orbit of epoch on the ICRF equator, as in, e.g., Konopliv et al. (2016).

If we assume a solution in obliquity/longitude of the form (14a, 14b), then the equatorial coordinates can be written as

$$\alpha = \alpha_0 + \dot{\alpha}t + \frac{\ddot{\alpha}}{2}t^2 + \Delta\alpha, \tag{23a}$$

$$\delta = \delta_0 + \dot{\delta}t + \frac{\ddot{\delta}}{2}t^2 + \Delta\delta. \tag{23b}$$

The integration constants α_0 and δ_0 derive directly from observations. The integration constants in obliquity (ε_0) and longitude ($\psi_0 = \theta_0$) can then be determined from (α_0, δ_0) and $(\Omega_0, i_0, \varepsilon_{\text{Earth}})$ or (J, N). To express the recomputed RMAN99 series in Sect. 4.1 in terms of right ascension and declination, we will use the values $\alpha_0 = 317°.681$ and $\delta_0 = 52°.886$ of Davies et al. (1989), consistent with the obliquity and longitude integration constants used by Roosbeek (1999) [see their Eq. (3)]. In Sects. 4.2 and 4.3, to update the nutation series, we will consider the values $(\alpha_0, \delta_0) = (317°.6811155, 52°.8863525)$ of Konopliv et al. (2016).[12]

The variations in right ascension and declination are obtained as

$$\{\dot{\alpha}, \ddot{\alpha}, \Delta\alpha\} = \Gamma_{\alpha\varepsilon}\{\dot{E}, \ddot{E}, \Delta\varepsilon\} + \Gamma_{\alpha\psi}\{\dot{\Psi}, \ddot{\Psi}, \Delta\psi\}, \tag{24a}$$

$$\{\dot{\delta}, \ddot{\delta}, \Delta\delta\} = \Gamma_{\delta\varepsilon}\{\dot{E}, \ddot{E}, \Delta\varepsilon\} + \Gamma_{\delta\psi}\{\dot{\Psi}, \ddot{\Psi}, \Delta\psi\}. \tag{24b}$$

The values of the Γ coefficients, obtained from $(\alpha_0, \delta_0, \Omega_0, i_0, \varepsilon_{Earth})$, can easily be estimated, assuming that the variations in α and δ are small quantities:

$$\Gamma_{\alpha\varepsilon} = 1.135458\,(1.135478), \tag{25a}$$

$$\Gamma_{\alpha\psi} = 0.513838\,(0.513834), \tag{25b}$$

$$\Gamma_{\delta\varepsilon} = -0.728413\,(-0.728407), \tag{25c}$$

$$\Gamma_{\delta\psi} = 0.291631\,(0.291632). \tag{25d}$$

The first set of values will be used for the recomputation of the RMAN99 precession/nutation solution, whereas the values in parentheses will be used for the computation of the updated BMAN20 solution.

3.3.4 Cautions

Potential users of the nutation series should proceed with care. The chosen orientation of the equatorial plane of the IF, here the J2000 Mars mean orbit derived from a VSOP theory, affects the values obtained for the angles θ_0 and ε_0 (Fig. 4), which intervene in the computation of

[12] Note that they give the values of the integration constants in obliquity and longitude, but referred to the 1980 mean orbit. With their values for the angles J and N, orienting the 1980 orbit with respect to ICRF, we retrieve the observed values for α_0 and δ_0, from which we will obtain again the integration constant in obliquity and longitude, but this time referred to the J2000 mean orbit ($\varepsilon_0 = 25°.191819740$ and $\theta_0 = 35°.497525780$).

the nutation amplitudes. For consistency, the fundamental arguments to be used with the nutation series must be those of the orbital theory used to obtain θ_0 and ε_0. As an illustration of the potential error, we consider the different values for the mean longitude Ma of Mars in VSOP87:

$$Ma_{\mathrm{VSOP87}} = 355°.433 + 191402°.9930T, \tag{26}$$

and in the JPL *Keplerian Elements for Approximate Positions of the Major Planets*[13]:

$$Ma_{\mathrm{JPL}} = 355°.447 + 191403°.0268T, \tag{27}$$

with T the time measured in thousands of Julian years from J2000. Using Ma_{JPL} instead of Ma_{VSOP87} to compute the semi-annual term in Table 1 produces differences up to 0.5 mas in the time domain, due to the 0°.014 difference in the epoch value of Ma; and up to 0.03 mas after 20 years, due to the 0.03° difference in mean motion per thousand of years.

Depending on the users' preferences, the representation for $\Delta\psi$ and $\Delta\varepsilon$ can be modified. The J2000 values φ_j^0 of the arguments can be extracted from the cosine and sine functions, affecting the definition of the amplitudes:

$$\begin{Bmatrix} \Delta\psi \\ \Delta\varepsilon \end{Bmatrix} = \sum_j \left(\begin{Bmatrix} \tilde{\psi}_j^c \\ \tilde{\varepsilon}_j^c \end{Bmatrix} \cos f_j t + \begin{Bmatrix} \tilde{\psi}_j^s \\ \tilde{\varepsilon}_j^s \end{Bmatrix} \sin f_j t \right), \tag{28a}$$

$$\tilde{\psi}_j^c = \psi_j^c \cos\varphi_j^0 + \psi_j^s \sin\varphi_j^0, \tag{28b}$$

$$\tilde{\psi}_j^s = -\psi_j^c \sin\varphi_j^0 + \psi_j^s \cos\varphi_j^0, \tag{28c}$$

$$\tilde{\varepsilon}_j^c = \varepsilon_j^c \cos\varphi_j^0 + \varepsilon_j^s \sin\varphi_j^0, \tag{28d}$$

$$\tilde{\varepsilon}_j^s = -\varepsilon_j^c \sin\varphi_j^0 + \varepsilon_j^s \cos\varphi_j^0. \tag{28e}$$

This alternative representation can be rewritten as a pure sine (or cosine) representation, with phase values for the arguments depending not only on the chosen orbital theory but also on the rotation response of Mars itself:

$$\begin{Bmatrix} \Delta\psi \\ \Delta\varepsilon \end{Bmatrix} = \sum_j \begin{Bmatrix} \tilde{\tilde{\psi}}_j \sin(f_j t + \tilde{\tilde{\varphi}}_j^{\psi}) \\ \tilde{\tilde{\varepsilon}}_j \sin(f_j t + \tilde{\tilde{\varphi}}_j^{\varepsilon}) \end{Bmatrix}, \tag{29a}$$

$$\tilde{\tilde{\psi}}_j = \sqrt{(\tilde{\psi}_j^c)^2 + (\tilde{\psi}_j^s)^2}, \tag{29b}$$

$$\tilde{\tilde{\varepsilon}}_j = \sqrt{(\tilde{\varepsilon}_j^c)^2 + (\tilde{\varepsilon}_j^s)^2}, \tag{29c}$$

$$\tilde{\tilde{\varphi}}_j^{\psi} = \arctan \tilde{\psi}_j^c / \tilde{\psi}_j^s, \tag{29d}$$

$$\tilde{\tilde{\varphi}}_j^{\varepsilon} = \arctan \tilde{\varepsilon}_j^c / \tilde{\varepsilon}_j^s. \tag{29e}$$

Alternative representations can also be obtained for the pro/retro and right ascension/declination representations. For instance, Kuchynka et al. (2014) provide nutations series in (α, δ) in the pure sine form.

An advantage of those alternative representations is that their use is less prone to errors since the epoch values of the fundamental arguments are implicitly taken into account, even though care must be taken in using the correct frequencies of the arguments. This being said, for the sake of continuity with respect to RMAN99, we continue here with the first representation, as in Eq. (15).

[13] https://ssd.jpl.nasa.gov/?planet_pos.

3.4 Precession and nutations induced by the solar torque

The precession and nutations induced by the solar torque, assuming Mars on a Keplerian orbit of given orbital elements, can be expressed in analytical form to high order in eccentricity (RK79, Hilton 1991). Because of the mutual perturbations of the planets, the orbit of Mars is better described as an osculating orbit. Some efforts have been made to introduce the effects of the secular variations of the osculating elements in an analytical precession/nutation model. For instance, RK79 discussed the effect of the mean precession of Mars pericenter on the semi-annual nutation (see the end of the section "Principal Solar Terms" in their Appendix B). Hilton (1991) considered the effects of the secular variations in eccentricity, but used an incorrect procedure (see Sect. 2). He also tried to take into account the secular variations of the orbital inclination and node longitude. However, he used for this a different set of governing equations, taken from Ward (1974) and intended for study the climate of Mars, not for interpretation of lander data.[14]

It is possible to introduce in a consistent way the effects of the secular variations of all osculating elements in an analytical precession/nutation model, as we explain below. In reality, osculating elements are also varying periodically and a semi-analytical solution in the form of series (e.g., RMAN99 and BMAN20, see Sects. 4.1, 4.3) based on a semi-analytical orbital theory for the position of Mars is definitely more accurate than an analytical solution. Despite its limited accuracy, an analytical solution is still useful though to better understand the semi-analytical solution and assess the order of magnitude of individual effects. We here explain the basics of how precession and nutation terms can be obtained assuming Mars on an osculating orbit with secularly varying elements, without giving the full expression of the solution. We start from the expression for the coordinates of the Sun in the equinox BF, to be introduced in the AM Eqs. (12a, 12b):

$$\begin{pmatrix} X_S \\ Y_S \\ Z_S \end{pmatrix} = \mathbf{R_x}(\varepsilon_M)\cdot\mathbf{R_z}(\theta_M)\cdot\mathbf{R_x}(i_0)\cdot\mathbf{R_z}(\Omega_0-\Omega_M)\cdot\mathbf{R_x}(-i_M)\cdot\mathbf{R_z}(-\omega_M+\pi-\nu_M)\cdot\begin{pmatrix} r_S \\ 0 \\ 0 \end{pmatrix}, \tag{30}$$

with angles as defined in Fig. 4. The distance between the mass centers of Mars and the Sun, r_s, and the true anomaly of Mars, ν_M, can be expressed as

$$r_S = a_M - a_M e_M \cos M_M + \mathcal{O}(e_M^2), \tag{31a}$$

$$\nu_M = M_M + 2e_M \sin M_M + \mathcal{O}(e_M^2), \tag{31b}$$

with the mean anomaly $M_M = Ma - \Omega_M - \omega_M$ in which Ma is the mean longitude of Mars, and the argument we chose to express the solution.

3.4.1 Zero-order solution (main solar terms)

The solution is obtained iteratively. We first neglect the variations of ε_M, θ_M, i_M, Ω_M, ω_M, a_M and e_M in the right-hand members of the AM equations, and use their epoch values ε_0, θ_0, i_0, Ω_0, ω_0, a_0 and e_0, to obtain the zero-order solution. Under this assumption, we get

$$\begin{pmatrix} X_S \\ Y_S \\ Z_S \end{pmatrix} \simeq r_S \begin{pmatrix} -\cos(\theta_0-\omega_0-\nu_M) \\ \cos\varepsilon_0 \sin(\theta_0-\omega_0-\nu_M) \\ -\sin\varepsilon_0 \sin(\theta_0-\omega_0-\nu_M) \end{pmatrix}, \tag{32}$$

[14] In Ward's model, nutations are expressed with respect to the orbit of the date (see also the complementary term in the Hamiltonian of BS99 to account for the motion of the orbit of date, resulting in additional secular variations of the longitude and obliquity of Mars BF), and not to the orbit of a chosen epoch.

with $r_S = a_0 - a_0 e_0 \cos M_M + \mathcal{O}(e_0^2)$ and $\nu_M = M_M + 2e_0 \sin M_M + \mathcal{O}(e_0^2)$. Equations (12a, 12b) then show that $\dot{\psi}$ and $\dot{\varepsilon}$ are proportional to $1-\cos 2(\theta_0 - \omega_0 - \nu_M)$ and $\sin 2(\theta_0 - \omega_0 - \nu_M)$, respectively.

For $e_0 = 0$, the constant term in $\dot{\psi}$ leads, after integration, to a precession in longitude, whereas the cosine and sine terms in $\dot{\psi}$ and $\dot{\varepsilon}$ lead to the semi-annual nutation ($\sim 200 \cos 2Ma - 1100 \sin 2Ma$, with amplitudes in mas). For $e_0 \neq 0$, the precession rate in longitude due to the solar torque is given by (RK79):

$$\dot{\Psi}_S = -\frac{3}{2}\frac{n^2}{\Omega_R}(1-e_0^2)^{-3/2} H_D \cos\varepsilon_0, \tag{33}$$

and nutations at other periods (annual, ter-annual, ...) are obtained after trigonometric manipulations of the terms in $\dot{\psi}$ and $\dot{\varepsilon}$, besides the semi-annual nutations. The zero-order solution does not lead to secular variations in obliquity (the secular variation rate in obliquity due to the solar torque $\dot{E}_S = 0$).

3.4.2 First-order solution (planetary perturbations)

The first-order solution is obtained by introducing the secular variations $\dot{E}, \dot{\theta}_M = \dot{\Psi}, \dot{i}_M, \dot{\Omega}_M, \dot{\omega}_M, \dot{a}_M$ and $\dot{e}_M$ of the quantities $\varepsilon_M, \theta_M, i_M, \Omega_M, \omega_M, a_M$ and e_M, respectively, in the right-hand members of the AM equations[15] (12a, 12b). Linearizing the AM equations around the epoch values of these quantities, we identify two effects of the planetary perturbations: (1) quadratic terms in longitude and obliquity, and (2) secular variations of the nutation amplitudes.

The quadratic terms, at first order in i_0, are given by

$$\frac{\ddot{\psi}_S t^2}{2} = \frac{3H_D G M_S}{4\Omega_R a_S^4 \sin\varepsilon_0}\left(\frac{3}{2}\dot{a}_M \sin 2\varepsilon_0 - a_M \dot{E}\cos 2\varepsilon_0 + a_M \dot{i}_M \cos 2\varepsilon_0 \cos\theta_0 + a_M i_0 \dot{\Omega}_M \cos 2\varepsilon_0 \sin\theta_0\right) t^2, \tag{34a}$$

$$\frac{\ddot{E}_S t^2}{2} = -\frac{3H_D G M_S \cos\varepsilon_0}{4\Omega_R a_S^3}(-\dot{i}_M \sin\theta_0 + i_0 \dot{\Omega}_M \cos\theta_0) t^2. \tag{34b}$$

They amount to about $-13000\,T^2$ mas and $2000\,T^2$ mas, respectively, with T, the time measured in thousands of Julian years from J2000. The contributions from $\dot{a}_M$ and $\dot{E}$ are negligible compared to the contributions from $\dot{\Omega}_M$ and $\dot{i}_M$ to the quadratic variations in longitude. Those quadratic variations due to $\dot{\Omega}_M$ and $\dot{i}_M$ are found in RK79 with similar numerical values (see their equation B41 for $\ddot{\Psi} t^2/2$ and the value for $\ddot{E}$ after their equation C6).

The largest nutation amplitude variations are caused by the effect of the BF precession $\dot{\theta}_M$ [about $-80\,T$ mas on the cosine term and $+15\,T$ mas on the sine term of the semi-annual nutation, to be compared with the effect obtained in BMAN20 solution (Table 10)]. The cumulated effects of the secular variations of the osculating elements on the semi-annual nutation is about one order of magnitude smaller. This evaluation depends on the arguments chosen to express the solution (*Ma* here but M_M in RK79, explaining why we reach different conclusion regarding the importance of the effect of the orbit precession).

[15] The direct torque by the planets leads to a secular variation in obliquity $\dot{E}_{Pl}$, see Eq. 48b. This is why we do not necessarily assume here that $\dot{E} = 0$.

3.4.3 Geodetic precession and nutations

The planetocentric IF cannot be regarded as inertial from the relativistic point of view, as its origin is accelerated with respect to a solar system barycentric reference frame (Fukushima 1991, 2003). This effect generates a small but significant additional precession/nutation motion of the spin axis in space, called geodetic or geodesic precession/nutation. For the Earth, the precession rate in space is about $+50.288$ as/year, of which -0.019 as/year is attributed to geodetic precession rate (remember that for the Earth, the usual convention is to measure the longitude of the spin axis in the retrograde sense). Note that the sign of the geodetic precession rate is opposite to the sign of the lunisolar precession.

As the geodetic precession and nutations of Mars are expected to be small, it is sufficient to consider the orbit of Mars as Keplerian to estimate them. The geodetic contribution to the nutation in longitude, $\Delta\psi_g$, measured as a prograde angle can then be expressed as

$$\Delta\psi_g = \frac{3}{2c_L^2 a_0}\frac{GM_S}{(1-e_0^2)}(\nu_M + e_0 \sin \nu_M), \tag{35}$$

with c_L the speed of light (Fukushima 1991, see also Eq. 69 of Roosbeek and Dehant (1998)). By expressing the true anomaly at third order in eccentricity as

$$\nu_M = M_M + 2e_0 \sin M_M - \frac{1}{4}e_0^3 \sin M_M + \frac{5}{4}e_0^2 \sin 2M_M + \frac{13}{12}e_0^3 \sin 3M_M, \tag{36}$$

we get a geodetic precession rate $\dot{\Psi}_g$ of $+6.754$ mas/yr (with a sign opposite to that of $\dot{\Psi}_S \simeq -7600$ mas/yr), and geodetic nutations (in mas)

$$\begin{aligned}\Delta\psi_g = {} & 0.229 \cos Ma + 0.029 \cos 2Ma + 0.003 \cos 3Ma \\ & + 0.516 \sin Ma + 0.026 \sin 2Ma + 0.001 \sin 3Ma.\end{aligned} \tag{37}$$

Our estimated value for $\dot{\Psi}_g$ is consistent in magnitude with that estimated by RK79 (their Eq. B38) and BS99 (their Eq. 41). However, the sign of $\dot{\Psi}_g$ in RK79 is wrongly assumed to be negative in their text after their Eq. (8) where the total rate of precession is described. This sign error has propagated to Folkner et al. (1997b) and Konopliv et al. (2006), affecting the estimate of the polar moment of inertia from the observed precession rate, but not in Konopliv et al. (2011).

To the geodetic precession rate correspond the variations rates in right ascension and declination $\dot{\alpha}_g = 3.470$ mas/yr and $\dot{\delta}_g = 1.970$ mas/yr. In Sect. 4.3, we choose a truncation level of 0.025 mas in pro/retro amplitude. Therefore, only the annual term will be retained for the final solution BMAN20 and is included in Table 9.

3.5 Precession and nutations induced by Phobos and Deimos

Unlike for solar nutations terms, a simple analytical solution can be used to obtain the main nutations induced by Phobos and Deimos with a sufficient accuracy because they are smaller. BS99 considered a simple precessing orbit in their analytical solution, whereas RMAN99 used series for rectangular coordinates before integrating the AM equations. When the series are rescaled to the same satellite masses and scaling factor, both approaches are consistent within 0.01 mas (see Table 1) in nutation amplitudes. Hilton (1991) concluded that considering a simple circular precessing orbit is sufficient to obtain the satellite nutations terms.

Below, we derive an analytical solution in the Torque approach and demonstrate that, except for a secular term in longitude, it is equivalent to the solution of BS99 derived in the Hamiltonian approach.

The definition of the position vector $\mathbf{r}_P$ of Phobos involves different angles that are defined in Fig. 4. Phobos' orbit is precessing about the local Laplace plane, defined in order to minimize the variations in inclination i_P that is therefore considered as constant. With respect to the Laplace plane, the rate of variation of the ascending node longitude, $\dot{\Omega}_P$, is also considered as constant. The precession of Phobos' orbit is mainly driven by Mars and by the Sun so that the Laplace plane is lying between the orbital plane and equator of Mars, and follows the precession of the equator with respect to the orbit (Jacobson and Lainey 2014; Sinclair 1972). The constant inclination τ between the Laplace plane of Phobos and the equator of Mars (denoted ε in Jacobson and Lainey 2014) is $0^\circ.009$ for Phobos and $0^\circ.889$ for Deimos. We consider a circular orbit ($e_P = 0$, $r_P = a_P$ and $v_P = M_P$) and measure Ω_P from the common node of the Laplace plane and Mars equator on Mars orbit (from the node of the Laplace plane on the ICRF equator in Jacobson and Lainey (2014)). We also write the mean longitude $\lambda_P = \Omega_P + \omega_P + M_P = n_P t + \lambda_P^0$.

Correct up to the first order in inclination i_P and tilt τ, the coordinates of Phobos in the mean equinox BF[16] are then given by

$$\begin{aligned}\begin{pmatrix} X_P \\ Y_P \\ Z_P \end{pmatrix} &= \mathbf{R_x}(\tau)\cdot\mathbf{R_z}(-\Omega_P)\cdot\mathbf{R_x}(-i_P)\cdot\mathbf{R_z}(-\omega_P - M_P)\cdot\begin{pmatrix} a_P \\ 0 \\ 0 \end{pmatrix} \\ &= a_P\begin{pmatrix} \cos\lambda_P \\ \sin\lambda_P \\ -\tau\sin\lambda_P + i_P\sin(\lambda_P - \Omega_P) \end{pmatrix}. \end{aligned} \tag{38}$$

After integration of the AM equations (12a, 12b), the solution for the precession/nutation in longitude and in obliquity can be written as:

$$\begin{aligned}\Delta\psi = {} & \frac{-3H_D G M_P \tau}{2a_P^3\Omega_R\sin\varepsilon_0}\,t + \frac{3H_D G M_P i_P}{2a_P^3\Omega_R\dot{\Omega}_P\sin\varepsilon_0}\sin\Omega_p \\ & - \frac{3H_D G M_P i_P}{2a_P^3\Omega_R(2n_P - \dot{\Omega}_P)\sin\varepsilon_0}\sin(2\lambda_P - \Omega_P) + \frac{3H_D G M_P \tau}{4a_P^3\Omega_R n_P\sin\varepsilon_0}\sin 2\lambda_P, \end{aligned} \tag{39a}$$

$$\begin{aligned}\Delta\varepsilon = {} & \frac{3H_D G M_P i_P}{2a_P^3\Omega_R\dot{\Omega}_P}\cos\Omega_p - \frac{3H_D G M_P i_P}{2a_P^3\Omega_R(2n_P - \dot{\Omega}_P)}\cos(2\lambda_P - \Omega_P) \\ & + \frac{3H_D G M_P \tau}{4a_P^3\Omega_R n_P\sin\varepsilon_0}\cos 2\lambda_P. \end{aligned} \tag{39b}$$

This solution also applies to the nutations induced by Deimos after changing the coordinates of Phobos to Deimos.

The first periodic term in the solution (39a, 39b) is related to the period of nodal precession of the satellite (825.641 and 19998.9 days for Phobos and Deimos, respectively). Using the parameters' values from Table 2, we obtain nutation amplitudes of 9.882/4.388 mas in longitude and of −4.206/ − 1.868 mas in obliquity for Phobos/Deimos, very close to the values obtained in the RMAN99 recomputed series using ESAPHO and ESADE ephemerides

[16] The mean equinox BF is defined in Sect. 3.3, after Eqs. (16a, 16b). The transformation in Eq. 38 does not go to the mean equinox BF strictly speaking, but to a mean BF whose x-axis is in the direction of the node of the mean BF of date over the mean orbit of date (and not of epoch). Additional rotations can be introduced to account for this, but without noticeable effect on the solution.

Table 2 Parameter values used for recomputing RMAN99 series in Sect. 4.1, and meant to be consistent with VSOP87, ESAPHO, and ESADE theories

Parameter	Symbol (unit)	Value	References
Scaling factor[a]	H_D	0.00535464	RMAN99
Solar standard gravitational parameter	GM_S (m^3/s^2)	1.3271224×10^{20}	Table (1) of RMAN99, from McCarthy (1996)
Astronomical unit[b]	au (m)	149597870691	McCarthy (1996)
Constant of gravitation[c]	G ($m^3\,kg^{-1}\,s^{-2}$)	6.67259×10^{-11}	Ibid
Mean rotation rate of Mars	Ω_R (rad/s)	7.0882181×10^{-5}	Table (1) of RMAN99, from Chapront-Touze (1990), Davies et al. (1989)
Node longitude of Mars	Ω_0 (°)	49.55809321	Eq. (3) of RMAN99, with $t = 0$, from Simon et al. (1994)
Inclination of Mars	i_0 (°)	1.84972648	Ibid
Epoch node angle	θ_0 (°)	35.496817571	Eq. (3) of RMAN99, with $t = 0$, from Chapront-Touze (1990)
Obliquity of Mars	ε_0 (°)	25.192028020	Ibid
Obliquity of the Earth	$\varepsilon_{\text{Earth}}$ (°)	23.439280306	Bretagnon and Francou (1988)
Mass of Phobos	M_P (kg)	1.05×10^{16}	Table (1) of RMAN99, from Chapront-Touze (1990)
Mass of Deimos	M_D (kg)	1.80×10^{15}	Ibid
Longitude mean motion of Phobos	n_P (°/day)	1128.84476	Page 289-290 of BS99, from Chapront-Touze (1990)
Node longitude rate of Phobos	$\dot{\Omega}_P$ (°/day)	− 0.436025	ibid
Inclination of Phobos	i_P (°)	1.067639	Ibid
Semi-major axis of Phobos	a_P (km)	9373.713	Ibid
Longitude mean motion of Deimos	n_D (°/day)	285.161875	Ibid
Node longitude rate of Deimos	$\dot{\Omega}_D$ (°/day)	− 0.018001	Ibid
Inclination of Deimos	i_D (°)	1.78896	Ibid
Semi-major axis of Deimos	a_D (km)	23457.060	Ibid

The mean orbital elements of Phobos and Deimos are used to estimate the nutations induced by the satellites with an analytical solution (Eqs. 39a, 39b), and to compare them with the nutations obtained directly from the ESAPHO and ESADE ephemerides (Chapront-Touze 1990). The numerical values of the parameters for the computation of the BMAN20 series in Sect. 4.3 are given in Table 7

[a]The value of H_D used in Roosbeek (1999) was tuned to obtain the mean precession rate $\dot{\Psi} = -7576$ mas/yr of Folkner et al. (1997b), given the fact that using ephemerides instead of mean orbital elements alters the prediction made with the classical relation of Eq. (33) (Fabian Roosbeek, personal communication)

[b]Used to multiply the rectangular coordinates of the VSOP87

[c]Used to multiply the mass of Phobos and Deimos in Eqs. (39a, 39b)

(9.877/4.390 mas in longitude and −4.204/−1.863 mas in obliquity), confirming that an analytical theory is sufficiently accurate. The second and third periodic terms are at short period (approximately half the revolution period of the satellite, 0.16 days for Phobos, 0.63 days for Deimos) and have very small amplitudes (< 0.002 mas).

With $\tau = 0$, the analytical expressions of Eqs. (39a, 39b) are consistent with the analytical solution of BS99 (see their Eqs. 27.1–27.2). The terms proportional to τ are missing in Bouquillon and Souchay (1999) and Hilton (1991), because they assimilated the local Laplace plane with the equator of Mars. Though the nutation terms caused by τ are negligible, the secular term in precession (-0.232 mas/yr for Phobos and -0.250 mas/yr for Deimos) are of the same order as the direct effect of Jupiter as estimated in RK79, and should therefore intervene in the expression for the longitude precession. Note that we retrieve similar secular precession terms in RMAN99 recomputed series using ESAPHO and ESADE ephemerides (-0.232 mas/yr and -0.251 mas/y, see Sect. 4.1.2).

3.6 Precession and nutations induced by the planets (direct effect)

An analytical solution for the precession and nutations induced by the direct torque exerted by the other planets on Mars is discussed in Hilton (1991) for the case of circular orbits ($e = 0$) in a common plane ($i = 0$). Just as for the solar torque, it is possible to derive an analytical solution for the general Keplerian case. Although it is more accurate to consider series from semi-analytical orbital theories for the position of perturbating bodies before integrating the AM equations, we here provide the analytical solution in the case of Keplerian orbits, correct up to the first order in eccentricities and inclination. This will allow us to better understand the differences between the series solution of BS99, our series solution BMAN20 derived in Sect. 4.3.3, and the conclusions of RK79 regarding the direct effects of the planets.

By considering Keplerian orbits, the planet coordinates (subscript Pl) in the mean equinox BF are written as

$$\begin{aligned}\begin{pmatrix} X_{Pl} \\ Y_{Pl} \\ Z_{Pl} \end{pmatrix} &= \begin{pmatrix} X_S \\ Y_S \\ Z_S \end{pmatrix} \\ &+\mathbf{R_x}(\varepsilon_0)\cdot\mathbf{R_z}(\theta_0)\cdot\mathbf{R_x}(i_0)\cdot\mathbf{R_z}(\Omega_0-\Omega_{Pl}) \\ &\cdot\mathbf{R_x}(-i_{Pl})\cdot\mathbf{R_z}(-\omega_{Pl}-\nu_{Pl})\cdot\begin{pmatrix} r_{Pl} \\ 0 \\ 0 \end{pmatrix},\end{aligned} \tag{40}$$

with (X_S, Y_S, Z_S) the Sun coordinates as given in Eq. (30). Considering that the mean longitudes of the planet and Mars (and therefore the argument of the series to be built) are defined as

$$\lambda_{Pl} = \Omega_{Pl} + \omega_{Pl} + M_{Pl}, \tag{41a}$$

$$\lambda_M (= Ma) = \Omega_M + \omega_M + M_M, \tag{41b}$$

and that, to first order in eccentricities,

$$r_S = a_M - a_M e_M \cos M_M, \tag{42a}$$

$$r_{Pl} = a_{Pl} - a_{Pl} e_{Pl} \cos M_{Pl}, \tag{42b}$$

$$\nu_M = M_M + 2e_M \sin M_M, \tag{42c}$$

$$\nu_{Pl} = M_{Pl} + 2e_{Pl} \sin M_{Pl}, \tag{42d}$$

then the coordinates to first order in inclinations and eccentricities simplify to the form

$$\begin{pmatrix} X_{Pl} \\ Y_{Pl} \\ Z_{Pl} \end{pmatrix} = \begin{pmatrix} X_{Plo} \\ Y_{Plo} \\ Z_{Plo} \end{pmatrix} + \begin{pmatrix} \delta X_{Ple} \\ \delta Y_{Ple} \\ \delta Z_{Ple} \end{pmatrix} + \begin{pmatrix} \delta X_{Pli} \\ \delta Y_{Pli} \\ \delta Z_{Pli} \end{pmatrix}, \tag{43a}$$

with

$$\begin{pmatrix} X_{Plo} \\ Y_{Plo} \\ Z_{Plo} \end{pmatrix} = \begin{pmatrix} a_{Pl}\cos(\lambda_{Pl} - \Omega_M - \theta_0) - a_M\cos(\lambda_M - \Omega_M - \theta_0) \\ \cos\varepsilon_0(-a_{Pl}\sin(\lambda_{Pl} - \Omega_M - \theta_0) + a_M\sin(\lambda_M - \Omega_M - \theta_0)) \\ \sin\varepsilon_0(a_{Pl}\sin(\lambda_{Pl} - \Omega_M - \theta_0) - a_M\sin\varepsilon_0\sin(\lambda_M - \Omega_M - \theta_0)) \end{pmatrix}, \tag{43b}$$

$$\begin{aligned} \begin{pmatrix} \delta X_{Ple} \\ \delta Y_{Ple} \\ \delta Z_{Ple} \end{pmatrix} &= \begin{pmatrix} -\frac{1}{2}a_M e_M(\cos(\theta_0 - 2\lambda_M + \omega_M + 2\Omega_M) - 3\cos(\theta_0 - \omega_M)) \\ \frac{1}{2}a_M e_M\cos\varepsilon_0(\sin(\theta_0 - 2\lambda_M + \omega_M + 2\Omega_M) - 3\sin(\theta_0 - \omega_M)) \\ -\frac{1}{2}a_M e_M\sin\varepsilon_0(\sin(\theta_0 - 2\lambda_M + \omega_M + 2\Omega_M) - 3\sin(\theta_0 - \omega_M)) \end{pmatrix} \\ &+ \begin{pmatrix} \frac{1}{2}a_{pl}e_{Pl}\cos(\theta_0 - 2\lambda_{Pl} + \omega_{Pl} + \Omega_{Pl} + \Omega_M) \\ -\frac{1}{2}a_{pl}e_{Pl}\cos\varepsilon_0\sin(\theta_0 - 2\lambda_{Pl} + \omega_{Pl} + \Omega_{Pl} + \Omega_M) \\ \frac{1}{2}a_{pl}e_{Pl}\sin\varepsilon_0\sin(\theta_0 - 2\lambda_{Pl} + \omega_{Pl} + \Omega_{Pl} + \Omega_M) \end{pmatrix} \\ &+ \begin{pmatrix} -\frac{3}{2}a_{pl}e_{Pl}\cos(\theta_0 - \omega_{Pl} - \Omega_{Pl} + \Omega_M) \\ +\frac{3}{2}a_{pl}e_{Pl}\cos\varepsilon_0\sin(\theta_0 - \omega_{PL} - \Omega_{Pl} + \Omega_M) \\ -\frac{3}{2}a_{pl}e_{Pl}\sin\varepsilon_0\sin(\theta_0 - \omega_{PL} - \Omega_{Pl} + \Omega_M) \end{pmatrix}, \end{aligned} \tag{43c}$$

$$\begin{pmatrix} \delta X_{Pli} \\ \delta Y_{Pli} \\ \delta Z_{Pli} \end{pmatrix} = \begin{pmatrix} 0 \\ a_{Pl}\sin\varepsilon_0(i_{Pl}\sin(\lambda_{Pl} - \Omega_{Pl}) - i_M\sin(\lambda_{Pl} - \Omega_M)) \\ a_{Pl}\cos\varepsilon_0(i_{Pl}\sin(\lambda_{Pl} - \Omega_{Pl}) - i_M\sin(\lambda_{Pl} - \Omega_M)) \end{pmatrix}. \tag{43d}$$

Before substituting these expressions in Eqs. (12a, 12b), we first note that the squared distance between Mars and the planet does not depend on the inclinations at first order, and simplifies to:

$$d^2_{PlM} = d^2_{PlMo} + \delta(d^2_{PlM}), \tag{44a}$$

$$d_{PlMo} = \sqrt{a^2_{Pl} + a^2_S - 2a_{Pl}a_S\cos(\lambda_M - \lambda_{Pl})}, \tag{44b}$$

$$\begin{aligned} \delta(d^2_{PlM}) = &-2a^2_J e_J\cos(\lambda_{Pl} - \omega_{Pl} - \Omega_{Pl}) - 2a^2_M e_M\cos(\lambda_M - \omega_M - \Omega_M), \\ &-a_{Pl}a_M e_{Pl}(\cos(2\lambda_{Pl} - \lambda_M - \omega_{Pl} - \Omega_{Pl}) \\ &-3\cos(\lambda_M - \omega_{Pl} - \Omega_{Pl})) \\ &-a_{Pl}a_M e_M(\cos(\lambda_{Pl} - 2\lambda_M + \omega_M + \Omega_M) \\ &-3\cos(\lambda_{Pl} - \omega_M - \Omega_M)), \end{aligned} \tag{44c}$$

where $\delta(d^2_{PlM})$ is a quantity of first order in eccentricities. As a result the factor d^{-5}_{PlM} in Eqs. (12a, 12b) simplifies to:

$$d^{-5}_{PlM} = (d^2_{PlMo} + \delta(d^2_{PlM}))^{-5/2} = d^{-5/2}_{PlMo} - \frac{5}{2}\delta(d^2_{PlM})\, d^{-7/2}_{PlMo}, \tag{45}$$

so that

$$\begin{aligned} \dot{\psi} = 3H_D\frac{GM_{Pl}}{\sin\varepsilon_0\Omega_R}\Bigg(&\frac{Y_{Plo}Z_{Plo}}{d^5_{PlMo}} - \frac{5Y_{Plo}Z_{Plo}}{2d^7_{Plo}}\delta(d^2_{PlM}) + \frac{Y_{Plo}}{d^5_{PlMo}}(\delta Z_{Ple} + \delta Z_{Pli}) \\ &+\frac{Z_{Plo}}{d^5_{PlMo}}(\delta Y_{Ple} + \delta Y_{Pli})\Bigg), \end{aligned} \tag{46a}$$

$$\begin{aligned} \dot{\varepsilon} = 3H_D\frac{GM_{Pl}}{\Omega_R}\Bigg(&\frac{X_{Plo}Z_{Plo}}{d^5_{PlMo}} - \frac{5X_{Plo}Z_{Plo}}{2d^7_{Plo}}\delta(d^2_{PlM}) + \frac{X_{Plo}}{d^5_{PlMo}}(\delta Z_{Ple} \\ &+\delta Z_{Pli}) + \frac{Z_{Plo}}{d^5_{PlMo}}(\delta X_{Ple} + \delta X_{Pli})\Bigg). \end{aligned} \tag{46b}$$

The quantities d^{-5}_{PlMo} and d^{-7}_{PlMo} can be computed from Eq. (94) of Hilton, using Laplace coefficients $B^s_k(\alpha)$ (see also Eq. 22 of Laskar and Robutel 1995):

$$d^{-l}_{PlMo} = a_\alpha^{-l}\left(\frac{1}{2}B_0^{l/2}(\alpha) + \sum_{k>0} B_k^{l/2}(\alpha)\cos(k(\lambda_{Pl}-\lambda_M))\right), \tag{47a}$$

$$B^s_k(\alpha) = 2\frac{(s+k-1)!}{(s-1)!k!}\alpha^k F(s, s+k; k+1; \alpha^2), \tag{47b}$$

with $a_\alpha = \max(a_{Pl}, a_M)$, $\alpha = \min(a_{Pl}/a_M, a_M/a_{Pl})$, and F the Gaussian hypergeometric function. The expansion converges slowly for the Earth, because Mars and the Earth are relatively close to each other.

After inserting Eqs. (43b–43d) and (47a, 47b), (46a, 46b) for $\dot\psi/\dot\varepsilon$ are seen to contain constant terms $\dot\Psi_{Pl}$ and $\dot E_{Pl}$, which give rise to secular variations after integration, and periodic terms (nutations).

The rates of secular variations are given by

$$\begin{aligned}\dot\Psi_{Pl} = &-\frac{3H_D\cos\varepsilon_0 GM_{Pl}\left(a_{Pl}^2+a_M^2\right)B_0^{5/2}(\alpha)}{4a_\alpha^5\Omega_R} + \frac{3H_D\cos\varepsilon_0 GM_{Pl}a_{Pl}a_M B_1^{5/2}(\alpha)}{2a_\alpha^5\Omega_R}\\ &-\left(a_{Pl}B_0^{5/2}(\alpha) - a_M B_1^{5/2}(\alpha)\right)\\ &\frac{3H_D a_{Pl}GM_{Pl}\cos 2\varepsilon_0\left(i_M\cos\theta_0 - i_{Pl}\cos(\theta_0-\Omega_{Pl}+\Omega_M)\right)}{4a_\alpha^5\sin\varepsilon_0\Omega_R},\end{aligned} \tag{48a}$$

$$\begin{aligned}\dot E_{Pl} = &-\left(a_{Pl}B_0^{5/2}(\alpha) - a_M B_1^{5/2}(\alpha)\right)\\ &\frac{3H_D a_{Pl}GM_{Pl}\cos\varepsilon_0\left(i_M\sin\theta_0 - i_{Pl}\sin(\theta_0-\Omega_{Pl}+\Omega_M)\right)}{4a_\alpha^5\Omega_R}.\end{aligned} \tag{48b}$$

Those equations can be compared to previously published results. $\dot E_{Pl}$ and the third part of $\dot\Psi_{Pl}$ are proportional to the orbital inclinations i_{Pl} and i_M and are therefore not part of Hilton's solution. The second term in $\dot\Psi_{Pl}$, proportional to the Laplace coefficients $B_1^{5/2}$, results from the multiplication of terms proportional to $\cos(\lambda_{Pl}-\lambda_M)$ in d^{-5}_{Plo} and in the product Y_0Z_0, since $\cos^2(\lambda_{Pl}-\lambda_M) = (1+\cos 2(\lambda_{Pl}-\lambda_M))/2$. Such a term can be found in Hilton's solution (his Eq. 95), but is not included in his Eq. (24) for the precession in longitude, which contains only the first term proportional to $B_0^{5/2}$.

RK79 provides estimates for $\dot\Psi_{Pl}$ only, approximately obtained by a rescaling of the precession rate induced by the Sun, which is proportional to the solar mass and inversely proportional to the cube of the mean solar distance, to the mass and mean distance of the considered planet. This approximation can be found by neglecting the orbital inclinations, replacing a_α by a_{Pl}, and expanding to the order zero in α (so that $B_0^{5/2}\simeq 2$ and $B_1^{5/2}\simeq 0$):

$$\dot\Psi_{Pl} \simeq \dot\Psi_S\frac{M_{Pl}}{M_S}\left(\frac{a_S}{a_{Pl}}\right)^3. \tag{49}$$

The direct contributions of Jupiter, the Earth, Saturn, and Venus to the rates of secular variation are given in Table 3, and compared to the approximate solution of Eq. (49), the series solution of BS99, the series solution of Sect. 4.3.3, and Hilton's solution. Hilton's values are very different from the other values, and likely wrong for an unknown reason. RK79's approximation works very well for Saturn and fairly well for Jupiter, which are far enough from Mars so that the order 0 approximation in α is justified. The approximation

Table 3 Longitude and obliquity secular variations rates (in mas/yr) due to the direct torques by Jupiter, Saturn, the Earth, and Venus, obtained from an analytical solution, divided into the contributions from Laplace coefficients $B_0^{5/2}$ and $B_1^{5/2}$ (with $i_M = i_{Pl} = 0$) and from the inclinations i_M and i_{Pl} (columns 2–5)

Planet	$B_0^{5/2}$	$B_1^{5/2}$	i_M and i_{Pl}	Total	Approx RK79	BMAN20	BS99	Hilton
$(\dot{\Psi}_{Pl})$								
Jupiter	−0.323	0.114	−0.002	−0.221	−0.179	−0.223	−0.222	−0.198
Saturn	−0.010	0.001	0.000	−0.009	−0.009	−0.010	–	–
Earth	−0.618	0.540	0.004	−0.074	−0.080	−0.074	−0.082	−0.363
Venus	−0.094	0.062	−0.001	−0.033	−0.171	−0.034	–	–
$(\dot{E}_{Pl})$								
Jupiter	–	–	−0.006	−0.006	–	−0.0063	−0.0060	–
Saturn	–	–	−0.0004	−0.0004	–	−0.0002	–	–
Earth	–	–	0.0018	0.0018	–	0.0035	0.0025	–
Venus	–	–	0.00014	0.00014	–	0.0002	–	–

The rates obtained with the approximation of RK79 (Eq. 49), the series solution of Sect. 4.3.3, the series solution of BS99, and Hilton's solution are given in columns (6–9)

seems to work for the Earth, but it is by chance, as the approximation does not make sense in the first place for a planet closer to the Sun than Mars (it can be verified that it does not work at all for Venus). The agreement between the analytical solution and the BMAN20 solution is good, especially for the secular rate in longitude. For the smaller secular rate in obliquity, agreement is more difficult to reach, likely because of the approximations made in order to get the analytical solution.

The main nutations due to the planets are given in Table 4, and compared to the series solution of BS99 and the series solution BMAN20 of Sect. 4.3.3. For a truncation level of 0.025 mas in prograde/retrograde motion, as applied in Sects. 4.1 and 4.3, we find two terms for Jupiter, two terms for the Earth, and one term for Venus. For Jupiter, the agreement between the analytical solution and the series solution is again excellent. The agreement is good for the Earth and Venus. It is interesting to note that the Jupiter solution corresponds to BS99 solution only when we neglect the orbital inclination of the planets.

3.7 Oppolzer terms and polar motion

In the context of rotation studies, three axis are of interest: the figure, angular momentum (AM), and spin axes. The separation between the spin and figure axes is classically called *polar motion*. RK79 noticed that the misalignment between the figure and spin axes induced by the solar torque is small (about 5 cm at the surface of Mars, or 3 mas). The amplitude of the offset between the spin and AM axes is about[17] mH_D with m the amplitude of polar motion and H_D the scaling factor of Eq. (11c), and is two to three orders of magnitude smaller than the polar motion, so that the AM and spin axes can be assimilated to each other (BS99, RMAN99). In the following, by abuse of terminology, we will call *polar motion* the differential motion of the AM/spin axis with respect to the figure axis, as seen from the rotating Body Frame. We will call *Oppolzer terms* the differential motion of the figure

[17] Consider Eqs. (41) and (45) of Roosbeek and Dehant (1998), and the relation $N_{fH} = N_{rh} - m$, to get $N_{rH} = mH_D/(1 + H_D) \simeq mH_D$.

Table 4 Main nutations raised by the planets (direct effect) as obtained with an analytical solution, compared with the series solution of BS99 and the series solution of Sect. 4.3.3 (BMAN20)

j	Solution	Ju	Ma	Te	Ve	$2\pi/f_j$ (d)	ψ_j^c (mas)	ψ_j^s (mas)	ε_j^c (mas)	ε_j^s (mas)
Jupiter										
1	BS99	2	0	0	0	2166.29	−0.03	−0.19	−0.09	0.02
	Analytical						−0.042	−0.187	−0.088	0.021
	(with $i_M = i_{Pl} = 0$						−0.033	−0.187	−0.088	0.015
	BMAN20						−0.042	−0.187	−0.088	0.022
2	Analytical	−3	1	0	0	1310.24	0.018	−0.080	0.038	0.009
	BMAN20						0.018	−0.079	0.037	0.009
Earth										
1	BS99	0	2	−1	0	5764.01	−0.08	−0.14	0.00	0.00
	Analytical						−0.072	−0.127	0.000	0.000
	BMAN20						−0.076	−0.129	0.006	0.001
2	Analytical	0	4	−2	0	2882.00	−0.010	−0.080	−0.037	0.004
	BMAN20						−0.012	−0.078	−0.029	0.006
Venus										
1	Analytical	0	−3	0	1	11987.20	0.024	−0.146	0.069	0.011
	BMAN20						0.034	−0.150	0.066	0.012

axis with respect to the AM/spin axis, as seen from the Inertial Frame. Here, polar motion and Oppolzer terms have therefore opposite amplitudes, and different frequencies (a polar motion at frequency w in the rotating BF corresponds to an Oppolzer term at frequency $f = w + \Omega_R$ in the IF), but they represent in fact the same motion and have the same physical causes. The polar motion of Mars is mainly due to the atmospheric dynamics and the condensation/sublimation cycles of the atmosphere and polar ice caps. The amplitudes of the seasonal terms are expected to range between 0 and 15 mas (Defraigne et al. 2000; Van den Acker et al. 2002). The atmosphere can also excite the Chandler wobble, a normal mode for the motion of the spin axis with respect to the figure axis. The period of the Martian Chandler wobble is expected to be around 200 days, and its amplitude can be of the order of 10 to 100 mas (Dehant et al. 2006). The modeling of the atmospheric polar motion and of the Chandler wobble is beyond the scope of this study. As in RK79 and BS99, we consider that the polar motion/Oppolzer terms here are only due to the external gravitational torque.

It is possible to express the Oppolzer terms in terms of the nutations, since the motion of the figure axis in space and the motion of the spin axis in the BF are linked by the Euler kinematic equation

$$\dot{\varepsilon} + I\,\dot{\psi}\sin\varepsilon = (\omega_1 + I\omega_2)e^{I\phi}, \tag{50}$$

with $I = \sqrt{-1}$, which can be derived from Eq. (5b), and where (ψ, θ, ϕ) are the **Euler angles of the figure axis**. This equation can be rewritten in an alternative form using the prograde/retrograde formulation of the nutation series, as we show now. First, we use the simple fact that the motion of the unit vector $\hat{p}$ along the perpendicular to the inertial J2000 mean BF equator is not subject to any torque:

$$\frac{\mathrm{d}\hat{p}}{\mathrm{d}t} + \boldsymbol{\Omega} \wedge \hat{p} = 0. \tag{51}$$

Second, we find that, at first order in small variations,

$$\hat{p} = \mathbf{R_z}(\phi) \cdot \mathbf{R_x}(\varepsilon) \cdot \mathbf{R_z}(\psi - \psi_0) \cdot \mathbf{R_x}(-\varepsilon_0) \cdot \begin{pmatrix} 0 \\ 0 \\ 1 \end{pmatrix} = \mathbf{R_z}(\phi) \cdot \begin{pmatrix} -\delta x \\ -\delta y \\ 1 \end{pmatrix}, \tag{52}$$

for the component of $\hat{p}$ in the coordinates of Mars rotating BF, with (δ_x, δ_y) the projection of the trajectory of a unit vector along the figure axis on the J2000 mean BF equator (see Eq. 17). Finally, assuming that the projections $\mathbf{p} = \hat{p} - (0, 0, 1)$ and $\mathbf{m} = \boldsymbol{\Omega}/\Omega_R - (0, 0, 1) = (\omega_1, \omega_2, 0)/\Omega_R$ on the BF equator are circular motions at a common frequency $w = f - \Omega_R$ in the BF, that is to say that $p_x + Ip_y = pe^{Iwt}$ and $m_x + Im_y = me^{Iwt}$ with p the amplitude of the inertial pole motion, and m the amplitude of the polar motion, Eq. (51) becomes (Mathews et al. 1991):

$$p = \frac{m}{1 + w/\Omega_R}. \tag{53}$$

From Eqs. (18) and (52), $p = -\mathcal{A}_f$ with $\mathcal{A}_f$ the prograde ($\mathcal{P}_f$) or retrograde ($\mathcal{R}_f$) amplitude of the figure axis nutation, and Eq. (53) becomes

$$m_o = \mathcal{A}_f \frac{f}{\Omega_R}, \tag{54}$$

with $m_o = -m$ the amplitude of the Oppolzer terms (here the offset between the figure and spin axes, assimilated to the offset between the figure and AM axes). If we note $\mathcal{A}_S$ the amplitude of the spin axis nutation at frequency f in the IF, which is by definition the difference of the figure axis nutation and Oppolzer term amplitudes ($\mathcal{A}_f - m_o$) at the same frequency, we alternatively have that

$$m_o = \mathcal{A}_S \frac{f}{\Omega_R - f}. \tag{55}$$

From Eqs. (53–55), it follows that

$$\mathcal{A}_S = m \frac{\omega}{\omega + \Omega_R}, \tag{56a}$$

$$\frac{\mathcal{A}_f}{\Omega_R} = \frac{\mathcal{A}_S}{\Omega_R - f}. \tag{56b}$$

From Eq. (55), it is possible to find the amplitude of the Oppolzer terms corresponding to any nutation term for the AM axis, by switching between the longitude/obliquity and prograde/retrograde circular formulations. Since $\dot{\psi} \ll \Omega_R$, it is reasonable to consider that the precession has no polar motion/Oppolzer term counterparts ($m_o \simeq 0$ and $A_f \simeq A_S$). The Oppolzer terms, in longitude/obliquity, corresponding to the main terms of our recomputed RMAN99 nutations series are given in Table 5, along with the Oppolzer terms obtained by BS99, and the differences between the "RK79 rescaled" and "RMAN99 recomputed" series of Table 1. For the semi-annual nutation, the Oppolzer terms can reach up to 4 mas. In general, the Oppolzer terms correspond well to the difference between the RK79 rescaled series for the figure axis and the RMAN99 recomputed series for the AM axis. The remaining differences can be attributed to the differences in the treatment of the orbital configuration of Mars (unperturbed Keplerian orbit of given orbital elements for RK79, orbit taken from the VSOP87 ephemerides for RMAN99).

Conversely, from Eq. (56a) and a model of the atmospheric polar motion, it is in principle possible to compute the amplitude of the corresponding (non-rigid) nutation of the AM axis in space. Let us consider a polar motion with an amplitude of 10 mas at annual period. The

Table 5 Differences (in mas) between the RK79 (rescaled) and RMAN99 (recomputed) series for the main solar terms of Table 1 (columns 2–3)

	RK79-RMAN99		RMAN99 Oppolzer		BS99 Oppolzer	
Arg.	cos	sin	cos	sin	cos	sin
$(\Delta\psi)$						
$1Ma$	-0.04	0.19	-0.04	0.17	-0.04	0.16
$2Ma$	-0.64	-3.66	-0.62	-3.57	-0.62	-3.55
$3Ma$	-0.61	-0.96	-0.66	-0.99	-0.66	-0.99
$4Ma$	0.18	-0.19	-0.23	-0.14	-0.23	-0.14
$5Ma$	-0.18	-0.05	-0.05	-0.01	0.	0.
$6Ma$	-0.07	0.02	-0.01	0.	0.	0.
$(\Delta\varepsilon)$						
$1Ma$	-0.33	0.19	-0.30	0.18	-0.37	0.16
$2Ma$	-1.40	0.24	-1.41	0.28	-1.37	0.24
$3Ma$	-0.34	0.23	-0.38	0.26	-0.38	0.26
$4Ma$	-0.05	0.08	-0.06	0.09	-0.05	0.08
$5Ma$	-0.00	0.04	0.	0.02	0.	0.
$6Ma$	-0.01	-0.03	0.	0.	0.	0.

Oppolzer terms (mas), in longitude/obliquity of the recomputed RMAN99 (columns 4–5) and the rescaled BS99 (columns 6–7) nutation series

corresponding AM nutations would have quasi diurnal periods in the IF, much shorter than the harmonics of the annual period related to the solar torque, and an amplitude of 0.015 mas.

4 Semi-analytical solution

In this section, we first recompute the nutation series of the AM axis of Roosbeek (1999) (RMAN99), considering the same original calculation settings since the computer performances available at the time of the computation of RMAN99 made the semi-analytical treatment tedious and less accurate than intended. As we will see below, the computational error on the semi-annual term was of about 0.3 mas, above the chosen truncation criterion of 0.1 mas. The recomputed series (**RMAN99 recomputed**) presents a negligible computational error, as demonstrated by a comparison with a numerical integration of the AM equations (**RMAN99num**).

In a second step, we use the planetary ephemerides from VSOP2000, VSOP2013, DE431, and INPOP17a to assess the effect of a change in ephemerides on the precession/nutation solution. We also evaluate the effect of the chosen values for the constants (e.g., H_D) involved in the computations. To update the nutations induced by Phobos and Deimos, we use the mean orbital elements of Jacobson and Lainey (2014) and the analytical solution of Sect. 3.5. We also consider the direct effects of the Earth, Jupiter, Saturn, Venus, and Mercury on the precession/nutation of Mars. The full solution (solar, satellites, and direct planetary terms) defines the **BMAN20** solution.

Finally, as not all terms of BMAN20 will be above the detection capabilities of the RISE and LaRa experiments, we provide a restricted version (BMAN20 for Radio-Science, or **BMAN20RS**) of the solution which includes only main solar terms (possibly merged with indirect planetary terms) and satellite terms. We also estimate the uncertainty on the individual terms of the solution, which mainly results from the uncertainty on the scaling factor H_D.

4.1 Recomputation of RMAN99

To estimate the nutations induced by the solar torque, Roosbeek (1999) integrates over time the AM Eqs. (12a, 12b). The distance d_B is directly taken from the VSOP87 as equal to d_M, the distance of Mars to the Sun. The position (X_B, Y_B, Z_B) of the Sun is expressed in a reference frame attached to the J2000 mean equinox BF[18] after the following transformation (see Fig. 4)

$$\begin{pmatrix} X_B \\ Y_B \\ Z_B \end{pmatrix} = \underbrace{-\mathbf{R_x}(\varepsilon_0)\cdot\mathbf{R_z}(\theta_0)\cdot\mathbf{R_x}(i_0)\cdot\mathbf{R_z}(\Omega_0)}_{\mathbf{MT}}\cdot\begin{pmatrix} x_M \\ y_M \\ z_M \end{pmatrix}, \tag{57}$$

with (x_M, y_M, z_M) as given in VSOP87 (Bretagnon and Francou 1988) for the position of Mars in a reference frame attached to the ecliptic (Earth orbit) and equinox (ascending node of the Earth orbit on the Earth equator) at the J2000 epoch. (x_M, y_M, z_M), (X_B, Y_B, Z_B), and d_M are written as series of the form

$$\sum_j \left(C_j \cos\varphi_j + S_j \sin\varphi_j\right), \tag{58a}$$

$$C_j = \sum_\alpha T^\alpha C_{\alpha,j}, \tag{58b}$$

$$S_j = \sum_\alpha T^\alpha S_{\alpha,j}, \tag{58c}$$

where $C_{\alpha,j}$ and $S_{\alpha,j}$ are amplitudes and T is the time measured in thousands of Julian years from J2000. φ_j are linear combinations of fundamental arguments. After integration of Eqs. (12a, 12b), the fundamental arguments of the nutation series of Eq. (15) are the same as the VSOP87 arguments, by construction (see also Sect. 4.1.1). The arguments needed to express the truncated solution will be the mean longitudes of Saturn (Sa), Jupiter (Ju), Mars (Ma), the Earth (Te), and Venus (Ve), see Table 2 of Bretagnon and Francou (1988):

$$Sa = 0.87401675650 + 213.2990954380\,T, \tag{59a}$$

$$Ju = 0.59954649739 + 529.6909650946\,T, \tag{59b}$$

$$Ma = 6.20347611291 + 3340.6124266998\,T, \tag{59c}$$

[18] Roosbeek (1999) took $t = 0$ in his Eq. (3) (Roosbeek, personal communication). Therefore, the transformation from the IF goes to the J2000 BF and not the BF of date.

$$Te = 1.75347045953 + 6283.0758499914\,T, \tag{59d}$$

$$Ve = 3.17614669689 + 10213.2855462110\,T. \tag{59e}$$

The power α is an integer in-between 0 and 5. For $\alpha = 0$, the series are periodic, like the periodic nutations series of Roosbeek (1999). For $\alpha \geq 1$, the series are pseudo-periodic (Poisson series) and were not computed in Roosbeek (1999). Therefore, we consider only $\alpha = 0$ to recompute RMAN99 series.

To estimate the nutations induced by Phobos and Deimos, Roosbeek (1999) integrates the AM Eqs. (12a, 12b) with the positions (X_P, Y_P, Z_P) and (X_D, Y_D, Z_D) of the natural satellites obtained directly in the mean equinox BF from the ephemerides ESAPHO and ESADE of Chapront-Touze (1990) without transformations ($\mathbf{MT} = I_3$ is an identity matrix). Their squared distances d_P^2 and d_D^2 can be obtained as $(X_P^2 + Y_P^2 + Z_P^2)$ and $(X_D^2 + Y_D^2 + Z_D^2)$, respectively. In ESAPHO and ESADE, the positions of the natural satellites are also defined as periodic series under the form (58a), considering a specific set of fundamental arguments. After integration, the arguments of the main terms related to Phobos and Deimos in the nutation series are the orbital nodes of the satellites (constructed from the argument combination $D - F + l' + \omega' *$ of Roosbeek 1999):

$$N_{Ph} = 125^\circ.8759 - 159257^\circ.97707018\,T, \tag{60a}$$

$$N_{De} = 11^\circ.1971 - 6574^\circ.96623684\text{‘}\,T. \tag{60b}$$

The values of the transformation angles $(\varepsilon_0, \theta_0, i_0, \Omega_0)$ in Eq. (57) are taken from Eq. (3) of Roosbeek (1999). Besides the transformation angles, the integration of the AM equations also requires values for $GM_{S,P,D}$, the Solar/Phobos/Deimos standard gravitational parameters, for Ω_R, the mean rotation rate of Mars, and for H_D, the scaling factor. Here, for consistency, we use the same values as Roosbeek (1999) (see Table 2).

4.1.1 Computational procedure

To obtain nutation series in the form of Eq. (15), it is preferable to express the right-hand members of the AM Eqs. (12a, 12b) in a similar form first. We now describe briefly this computational procedure.

Since d_M, the Sun–Mars distance, is the sum of a constant term d_o (1.53033 AU in VSOP87) and of series δd with terms of amplitudes $\ll d_o$, the ratio $1/d_M$ can be expanded about $1/d_o$ as follows

$$\frac{1}{d_M} = \frac{1}{(d_o + \delta d)} = \frac{1}{d_o} + \sum_{k\geq 1}^{k_{max}} (-1)^k \frac{(\delta d)^k}{d_o^{k+1}}. \tag{61}$$

The maximal value $k_{max} = 11$ is chosen such as to ensure that the computational uncertainty on the solution is negligible, as can be checked with a numerical integration of the AM equations (see Sect. 4.1.4). This expansion is then raised to the fifth power, before being multiplied by $Y_B Z_B$ or $X_B Z_B$.

The squared Mars–Phobos distance d_P^2 is the sum of a constant term d_{Po}^2 and of periodic terms $\delta(d_P^2)$, so we use the following expansion about d_{Po}^2:

$$\left(\frac{1}{d_P}\right)^5 = \left(\frac{1}{d_{Po}^2 + \delta(d_P^2)}\right)^{5/2} = \frac{1}{d_{Po}^5} - \frac{5\,\delta(d_P^2)}{2\,d_{Po}^7} + \frac{35\,(\delta(d_P^2))^2}{8\,d_{Po}^9} + \ldots \tag{62}$$

$1/d_P^5$ is then multiplied by $Y_P Z_P$ or $X_P Z_P$. The same procedure applies to Deimos.

At each calculation step, trigonometric manipulations are used to express quantities in a form similar to that of Eq. (58a), and we neglect the smallest terms, considering a relative tolerance which ensures the accuracy of the solution. In the end of this computational procedure, the AM equations are in the form

$$\left\{ \begin{array}{c} \frac{\mathrm{d}\Delta\psi}{\mathrm{d}t} \\ \frac{\mathrm{d}\Delta\varepsilon}{\mathrm{d}t} \end{array} \right\} = \sum_j \left(\left\{ \begin{array}{c} C_j^{\psi} \\ C_j^{\varepsilon} \end{array} \right\} \cos\varphi_j + \left\{ \begin{array}{c} S_j^{\psi} \\ S_j^{\varepsilon} \end{array} \right\} \sin\varphi_j \right). \tag{63}$$

4.1.2 Secular solution

For $j = 0$, the secular part of the solution of Eqs. (14a, 14b) is given by

$$\dot{\Psi}\, t = \dot{\Psi}_S\, t + \dot{\Psi}_P\, t + \dot{\Psi}_D\, t, \tag{64a}$$
$$\dot{E}\, t = \dot{E}_S\, t + \dot{E}_P\, t + \dot{E}_D\, t, \tag{64b}$$

with

$$\dot{\Psi}_S = -7578.132\,\text{mas/yr}\ ;\ \dot{E}_S = -0.002\,\text{mas/yr}, \tag{64c}$$
$$\dot{\Psi}_P = -0.232\,\text{mas/yr}\ ;\ \dot{E}_P = 0\,\text{mas/yr}, \tag{64d}$$
$$\dot{\Psi}_D = -0.251\,\text{mas/yr}\ ;\ \dot{E}_D = 0\,\text{mas/yr}. \tag{64e}$$

The rate of variations of the right ascension and declination, see Eqs. (24a, 24b), are therefore given by

$$\dot{\alpha} = -3894.186\,\text{mas/yr} = -1^{\circ}.082\,\text{/kyr}, \tag{65a}$$
$$\dot{\delta} = -2210.160\,\text{mas/yr} = -0^{\circ}.614\,\text{/kyr}. \tag{65b}$$

Contrary to the analytical solution (see Sect. 3.4.1), the secular rate in obliquity $\dot{E}_S \neq 0$, but is very small, and there are no quadratic terms in the recomputed RMAN99 solution, as we consider only $\alpha = 0$ in Eq. (58a). The difference between the recomputed and old values for $\dot{\Psi}_S$ (-7578.132 vs. -7576 mas/yr) is about 2 mas/year. The difference between the recomputed value and the precession rate (-7578.09 mas/yr) obtained with the analytical solution [Eq. (33)] is 0.04 mas/yr, one order of magnitude smaller than the expected precision ($\simeq 0.3$ mas/yr) on the precession rate from RISE and LaRa (Dehant et al. 2020). This shows that using an analytical method to infer H_D from the measured precession rate does not introduce a significant bias. We find a very small but nonzero secular variation rate in obliquity $\dot{E}$, due to the mutual perturbations of the planets. The effect of Phobos and Deimos on the precession rate of Mars (-0.232 mas/year and -0.251 mas/year) differ from the old values by less than 0.0005 mas/year (Fabian Roosbeek, personal communication) and compare very well with those obtained with the analytical solution (-0.232 mas/year and -0.250 mas/year, see Sect. 3.5).

4.1.3 Periodic series

For $j \geq 1$, the nutations in longitude and obliquity have amplitudes given by

$$\begin{pmatrix} \psi_j^c \\ \psi_j^s \\ \varepsilon_j^c \\ \varepsilon_j^s \end{pmatrix} = \frac{1}{\dot{\varphi}_j} \begin{pmatrix} -S_j^{\psi} \\ C_j^{\psi} \\ -S_j^{\varepsilon} \\ C_j^{\varepsilon} \end{pmatrix}, \tag{66}$$

with $C/S_j^{\psi/\varepsilon}$ coming from Eq. 63.

For practical reasons (we find several tens of thousands of terms in the solution for the periodic series, most of them are not relevant in practice), a truncation criterion needs to be defined for presenting the recomputed RMAN99 series. Originally, RMAN99 considered the same truncation criterion of 0.1 mas in both longitude and in obliquity. A truncation criterion in obliquity of $\sin\varepsilon_0 \times 0.1\,\text{mas} = 0.4\,\text{mas}$ could be considered more consistent with the truncation criterion in longitude, as it would correspond to similar surface displacements (note that RK79 chose 0.7 and 0.3 mas as the truncation criterion in longitude and obliquity, respectively). Here, we keep the terms which have prograde and/or retrograde amplitudes larger than 0.025 mas. In this way, we provide the obliquity terms corresponding to all the longitude terms retained, which was not the case in the original series RMAN99 in which there are 24 terms in longitude and 10 terms in obliquity. We end up with 34 solar terms, one term for Phobos, and one term for Deimos. The recomputed RMAN99 solution, using the three representations of the solution (longitude/obliquity, prograde/retrograde, right ascension/declination) defined in Sect. 3.2, is available at https://doi.org/10.24414/h5pn-7n71. In Table 6, we present the amplitudes in longitude and obliquity, as well as the prograde and retrograde amplitudes, of selected terms.

We recover all the terms of the original series, with the exception of the 24th term in longitude in Table II of Roosbeek (1999), whose amplitudes was artificially high because of the lack of accuracy of the computational procedure applied by RMAN99 for very long period terms (lower maximal value for k and larger relative tolerance than ours). We also find several new terms with amplitudes below the truncation criterion of Roosbeek (1999) and two long period terms (lines 35–36 in Table 6) with amplitudes larger that Roosbeek (1999) failed to identify. The differences between the original and recomputed RMAN99 series amounts to 0.3 mas in amplitude for the semi-annual term in longitude (see line 15 in Table 6 and line 10 in Table II of Roosbeek 1999). The difference between the recomputed and original Phobos and Deimos terms is only 0.02 mas at most (9.86 mas versus 9.88 in longitude, for the nutation due to Phobos). The last reason for the differences between the original and recomputed RMAN99 series results from the application of the truncation criterion in Roosbeek (1999), not only both in longitude and obliquity, but also both in cosine and sine terms. As Roosbeek (1999) writes the amplitude down to the second decimal, 40% of the solar terms in longitude and 12.5% of the solar terms in obliquity of RMAN99 are written down as 0.00 mas, and the reader cannot know which terms are really zero up to the second digit, and which terms are below the truncation criterion. As a consequence, terms with amplitudes as large as 0.085 mas (the sine amplitude of the seventh solar term, line 1 in Table 6 and in Table II of Roosbeek (1999)) were neglected.

4.1.4 Solution accuracy: effect of the computational procedure

To assess the accuracy of the series solution (we mean here the entire RMAN99 recomputed series, not the truncated series), we numerically integrate Eqs. (12a, 12b) over time, without applying the computational procedure presented in Sect. 4.1.1. The numerical solution RMAN99num is obtained as follows

$$\Delta\psi(t) = \Delta\psi(t_o) + \int_{t_o}^{t} \frac{\mathrm{d}(\Delta\psi)}{\mathrm{d}t}\mathrm{d}t, \tag{67a}$$

$$\Delta\varepsilon(t) = \Delta\varepsilon(t_o) + \int_{t_o}^{t} \frac{\mathrm{d}(\Delta\varepsilon)}{\mathrm{d}t}\mathrm{d}t, \tag{67b}$$

Table 6 Selected periodic terms (main solar terms, satellite terms, and long periods terms) of the RMAN99 recomputed series, using the longitude/obliquity and prograde/retrograde representations defined in Sect. 3.2

j		Sa	Ju	Ma	Te	Ve	N_{Ph}	N_{De}	$2\pi/f_j$(d)	ψ_j^c(mas)	ψ_j^s(mas)	ε_j^c(mas)	ε_j^s(mas)	$\mathcal{P}_j$(mas)	$\mathcal{R}_j$(mas)
1		0	0	7	0	0	0	0	98.140	−0.102	0.085	0.040	0.048	0.059	0.003
2		0	0	6	0	0	0	0	114.497	−0.893	0.253	0.117	0.419	0.415	0.020
3		0	0	5	0	0	0	0	137.396	−6.262	−0.885	−0.427	2.928	2.825	0.133
4		0	0	4	0	0	0	0	171.745	−34.832	−21.661	−10.209	16.193	18.301	0.843
7		0	0	3	0	0	0	0	228.993	−137.078	−200.058	−93.513	62.673	107.898	4.705
22		0	0	1	0	0	0	0	686.980	−282.484	−477.765	47.671	11.912	102.108	136.705
25	(P)	0	0	0	0	0	−1	0	825.642	0.000	9.877	−4.204	0.000	0.000	4.204
32	(D)	0	0	0	0	0	0	−1	19998.582	0.000	4.390	−1.863	0.000	0.000	1.866
33		5	−2	0	0	0	0	0	322614.503	−0.363	0.104	−0.143	0.075	0.125	0.101
34		0	−3	8	−4	0	0	0	651392.660	0.996	0.290	−0.003	0.013	0.214	0.227
35		5	4	−16	8	0	0	0	3.40948×10^7	0.137	0.189	0.028	−0.095	0.094	0.032
36		−6	8	−7	0	2	0	0	1.33011×10^8	0.080	0.455	−0.150	−0.132	0.086	0.179

The full solution is available at https://doi.org/10.24414/h5pn-7n71. The arguments $Sa, \ldots, N_{De}$ are given in Eqs. (59a–60b). The table contains terms which have prograde and/or retrograde amplitudes larger than 0.025 mas. The first seven main solar terms and the satellites terms are highlighted in blue and gray, respectively. They are used in Table 1 where RMAN99 recomputed series are compared with the main terms of RK79 and BS99 series

considering $t_o = J2018$ and t between $J2018$ and $J2023$. We set $\Delta\psi(t_o)$ and $\Delta\varepsilon(t_o)$ to the values obtained with the recomputed RMAN99 series, so that at t_o the differences are zero. The differences between the RMAN99num and the RMAN99 recomputed series result from the computational procedure applied to find a solution in the form of a series, and can be seen as a computational contribution to the uncertainty on the solution. As the differences in the time domain are very small (of the order of 10^{-5} mas at most within the 2018–2025 time period), this contribution can be safely neglected when the nutation amplitudes are written down to the third digit, as in Table 6.

4.2 How to update the nutations series?

We have already established in Sect. 3.5 that the use of an analytical solution and recent mean orbital elements is sufficient to update the nutations induced by Phobos and Deimos. In this section, we explore the three following components of the computation, that can affect the nutation series induced by the Sun:

1. The choice of ephemerides (VSOP87, VSOP2000, …),
2. The value of the transformation angles (Ω_0, i_0, θ_M and ε_0),
3. The value of the other constants involved in the AM equations (in particular H_D).

4.2.1 The choice of ephemerides

The VSOP ephemerides are analytical planetary theories, fitted to numerical integrations, themselves fitted to observations. VSOP87, VSOP2000 and VSOP2013 are fitted to DE200 (Standish 1982), DE403 (Standish et al. 1995), and INPOP10a (Fienga et al. 2011), respectively. In the VSOP2000 ephemerides, the Mars coordinates (x_M, y_M, z_M) are expressed in the same form as in VSOP87 (see Eq. 58a) and d_M can be computed as their norm. In VSOP2013, the rectangular coordinates (x_M, y_M, z_M) are given in the form of Tchebychev polynomials, from which time series can be produced, before computing numerically the

corresponding nutation time series. Nutation time series can also be obtained from DE431 and INPOP17a, the most recent American and European ephemerides.

VSOP2000 and VSOP87 ephemerides can be used with or without the Poisson terms of Eq. (58a). The difference in nutation time series obtained with and without the Poisson terms represents the effect of the mutual perturbations between the planets on the nutation series, which is of the order of the mas (between − 3 and 2 mas in longitude and − 0.3 and 0.7 mas in obliquity within the 2018–2025 time period), and should be included in an updated nutation solution. The nutation time series obtained with VSOP2013, DE431, or INPOP17a include the effect of the mutual perturbations between the planets.

Considering Poisson terms, and all other things (the values of the transformation angles and of the other constants) being unchanged, the differences in nutations time series obtained from VSOP2000 versus VSOP87 are small (e.g., about −0.0003 mas/yr in the precession rate and 0.0002 mas in amplitude for the semi-annual nutation), and therefore negligible. The differences in nutations times series obtained numerically from VSOP2000 versus VSOP2013 are even smaller. We also verified that the nutation time series based on VSOP2000 differ negligibly from numerical nutation solutions obtained from DE431 or INPOP17a (about −0.0016 mas/yr on the precession rate and 0.0004 mas in amplitude for the semi-annual nutation).

As is apparent from the above, we could in principle use indifferently VSOP87 or VSOP2000 periodic and Poisson series for the solar coordinates to update the nutation semi-analytical solution. However, the choice of the VSOP theory influences the definition of the mean orbital elements involved in the definition of the transformation angles which, as we will see below, have a significant effect on the solution. Mean orbital elements are not provided for VSOP2000, while series for the rectangular coordinates (x_M, y_M, z_M) are not provided for VSOP2013. Since the difference between VSOP2000 and VSOP2013 ephemerides is negligible for our purpose, we will update the nutations series in Sect. 4.3 by using transformation angles consistent with VSOP2013 and rectangular coordinates from VSOP2000.

4.2.2 The value of the transformation angles

Four angles (Ω_0, i_0, θ_0, and ε_0) are involved in the transformation of Eq. (57) from the J2000 Earth ecliptic reference frame to the J2000 mean Equinox BF. Ideally, as the BF is precessing and nutating, the solar coordinates should be expressed in the true BF of date, instead of the J2000 mean equinox BF, and expressions for θ and ε taking into account the precession and nutations should be used in the transformation. But since the precession/nutation is the motion we want to determine from the integration of the AM equation, those expressions are a priori unknown. A compromise is to express the solar torque in the mean equinox BF of date (that is to say still neglecting the nutation, see Sect. 3.4.1), assuming that we know a priori the precession rate in longitude of the BF with respect to the chosen reference plane, or $\dot{\theta}_M$. We do not introduce $\dot{E}$, the secular variation rate in obliquity, as its effect on the solution is negligible. The transformation of Eq. (57) is therefore replaced by

$$\mathbf{MT} = -\mathbf{R_x}(\varepsilon_0) \cdot \mathbf{R_z}(\theta_M) \cdot \mathbf{R_x}(i_0) \cdot \mathbf{R_z}(\Omega_0). \tag{68}$$

The values of Ω_0 and i_0 used by Roosbeek (1999) come from Simon et al. (1994). They are mean orbital elements consistent with VSOP87. To update the nutation series, we consider the mean orbital elements of Simon et al. (2013) that correspond to the VSOP2013, and in good approximation, to VSOP2000 (− 0.08 arcsec for Ω_0 and − 0.001 arcsec for i_0, compared to the values of Simon et al. 1994). The expression for θ_M and ε_M reported in

Table 7 Values of the parameters used to compute the solution BMAN20

Parameter	Symbol (Unit)	Value	Uncertainties	References
Scaling factor	H_D	0.00538017	0.00000148	Sect. 4.2.3
Solar standard gravitational parameter	GM_S (m^3/s^2)	$1.3271244002 \times 10^{20}$	$0.0000000010 \times 10^{20}$	Konopliv et al. (2016)
Astronomical unit	au (m)	149597870700	3	Ibid
Mean rotation rate of Mars	Ω_R (rad/s)	7.08822×10^{-5}	2.4×10^{-15}	Ibid, or Archinal et al. (2018)
Node longitude of Mars	Ω_0 (°)	49.55807197	Unknown	Simon et al. (2013)
Inclination of Mars	i_0 (°)	1.84972607	Unknown	Ibid
Obliquity of the Earth	$\varepsilon_{\text{Earth}}$ (°)	23.439280933	Unknown	Ibid
Epoch node angle	θ_0 (°)	35.497525780	0°.0000026	Sect. 3.4.3 and Konopliv et al. (2016)
Obliquity of Mars	ε_0 (°)	25.191819740	0°.0000043	Ibid

The values of the parameters specific to Phobos and Deimos are given in Table 8

Roosbeek (1999) come from Chapront-Touze (1990). We now use $\varepsilon_0 = 25°.191819740$ and $\theta_0 = 35°.497525780$, and $\dot{\theta}_M = \dot{\Psi} = -7608.3$ mas/yr, which are consistent with the latest determination of the spin axis orientation by Konopliv et al. (2016), see Sect. 3.4.3.

In the time domain, the differences related to the update of the J2000 values of the transformation angles are larger (up to 0.15 mas in longitude and 0.02 mas in obliquity within the 2018–2025 time period) than the differences related to the choice of ephemerides, and are mainly due to the update of θ_0 (which differs by 2.5 arcsec from the value consistent with VSOP87). The effect of $\dot{\theta}_M$ is of the same order (the mas) than the effect of the Poisson terms of the ephemerides.

4.2.3 The value of the other constants involved in the AM equations

The updated values for GM_S and Ω_R (Table 7) are very close to the previous values (Table 2) and the changes do not affect significantly the solution. On the contrary, updating the value of the scaling factor is needed for several reasons. Roosbeek (1999) chose the value for H_D in order to retrieve the measured $\dot{\Psi}$ of Folkner et al. (1997b) considering only the solar torque. We need to choose the value for H_D to be consistent with the most recent measurement of $\dot{\Psi}$ by Konopliv et al. (2016), considering not only the solar torque, but also the direct torques by the other planet, by Phobos and Deimos, the geodetic precession, and the effect of long period terms. Only the geodetic precession is not proportional to H_D, therefore:

$$\dot{\Psi}_{observed} = \dot{\Psi}_g + \frac{H_D}{0.00535464}(\dot{\Psi}_S + \dot{\Psi}_{LP} + \dot{\Psi}_P + \dot{\Psi}_D + \dot{\Psi}_{Pl})|_{H_D=0.00535464}. \quad (69)$$

As

- $\dot{\Psi}_S|_{H_D=0.00535464} = -7578.144$ mas/yr (see Sect. 4.3.1),
- $\dot{\Psi}_{LP}|_{H_D=0.00535464} = -0.002$ mas/yr (see Sect. 4.3.1),

- $\dot{\Psi}_P|_{H_D=0.00535464} = -0.234$ mas/yr (see Sect. 4.3.2),
- $\dot{\Psi}_D|_{H_D=0.00535464} = -0.200$ mas/yr (see Sect. 4.3.2),
- $\dot{\Psi}_{Pl}|_{H_D=0.00535464} = -0.340$ mas/yr (see Sect. 4.3.3),
- $\dot{\Psi}_g = +6.754$ mas/yr (see Sect. 3.4.3),

we find that $H_D = 0.00538017$ (+0.5% with respect to the value of Roosbeek 1999) ensures that $\dot{\Psi} = -7608.3$ mas/yr, the measured precession rate of Konopliv et al. (2016). The current uncertainty on H_D is directly related to the uncertainty of 2.1 mas/yr on $\dot{\Psi}$, so that $\sigma_{H_D} = 0.00000148$, or 0.03%. The resulting uncertainty on the precession/nutation solution (e.g., 0.30 mas in semi-annual amplitude with the current measurement precision, 0.04 mas with the expected measurement precision of RISE and LaRa) is larger than the modeling uncertainties resulting from the choice of the ephemerides.

The 0.5% change in H_D affects the nutation amplitude (5 mas for the semi-annual term, 1 mas for the annual term, …, in longitude) well above the expected measurement accuracy. The precession rate will be re-estimated by RISE and LaRa. For consistency, it will be appropriate to re-update the value of H_D from the observed $\dot{\Psi}$ by RISE/LaRa, and therefore the amplitude of the rigid nutation terms, before determining Mars interior properties from the observed nutations.

From Eq. (11c) and the unnormalized gravity coefficient $J_2 = (C - \bar{A})/\mathrm{MR}^2 = 0.00195661 \pm 2.82 \times 10^{-10}$ (MRO120D gravity field, Konopliv et al. 2016), we determine the normalized polar moment of inertia of Mars

$$\frac{C}{\mathrm{MR}^2} = \frac{J_2}{H_D} = 0.36367 \pm 0.00010. \tag{70}$$

The uncertainty on C/MR^2 results almost entirely from σ_{HD}.

4.3 BMAN20 solution

We now build an up-to-date semi-analytical solution for the precession and nutations of a rigid Mars. The total precession/nutation is the sum of different terms that are computed in the following subsections. We first compute the solar terms, including the geodetic and semi-diurnal nutations. Then, we compute the satellite and the direct planetary terms.

4.3.1 Solar terms

We now use VSOP2000 ephemerides to update the solar terms of RMAN99 solution. The semi-analytical computational procedure is pretty much the same as with VSOP87 ephemerides. We integrate the AM Eqs. (12a, 12b). The position (X_B, Y_B, Z_B) of the Sun in the J2000 mean equinox BF is given by

$$\begin{pmatrix} X_B \\ Y_B \\ Z_B \end{pmatrix} = \mathbf{MT} \begin{pmatrix} x_M \\ y_M \\ z_M \end{pmatrix}, \tag{71}$$

with **MT** given by Eq. (68), and the values of the transformation angles are taken as explained in Sect. 4.2.2. In particular, θ_M varies with time, and $\dot{\theta}_M$ is taken as the measured rate of the precession in longitude. For the semi-analytical resolution, the transformation of Eq. (71) is expressed as series of $\dot{\theta}_M$.

In VSOP2000, Mars coordinates (x_M, y_M, z_M) are expressed in the same form as in VSOP87, with periodic and Poisson series (see Eq. 58a), but with a slightly different set

of fundamental arguments. The values of the five arguments used in the truncated nutation series are:

$$Sa = 0.87401678345 + 213.2990797783\,T, \tag{72a}$$
$$Ju = 0.59954667809 + 529.6909721118\,T, \tag{72b}$$
$$Ma = 6.20349959869 + 3340.6124347175\,T, \tag{72c}$$
$$Te = 1.75346994632 + 6283.0758504457\,T, \tag{72d}$$
$$Ve = 3.17613445715 + 10213.2855473855\,T. \tag{72e}$$

Here, we also consider Poisson series (we take $\alpha = 0$ and 1 in Eq. 58a) in the solution. Contrary to VSOP87, VSOP2000 does not include a series for the distance d_M between Mars and the Sun. We therefore create such a series for d_M^2 from the rectangular coordinates series, and use an expansion similar to Eq. (62).

After trigonometric manipulations, the AM equations can be written in the form of Eq. (63), with

$$C_j^{\psi/\varepsilon} = \sum_\alpha T^\alpha C_{\alpha,j}^{\psi/\varepsilon}, \tag{73a}$$
$$S_j^{\psi/\varepsilon} = \sum_\alpha T^\alpha S_{\alpha,j}^{\psi/\varepsilon}. \tag{73b}$$

Together with the mean precession rate $\dot\theta_M$, the Poisson series in (x_M, y_M, z_M) lead to quadratic variations and to Poisson nutation series, also called *mixed terms* in BS99, but also to a very small alteration of the periodic nutation series (largest effect smaller than 0.02 mas on the amplitude of the annual nutation in longitude).

For $j = 0$, the secular part of the solution is given by (in mas, and T is the time measured in thousands of years from J2000)

$$\psi = \sum_\alpha \frac{T^{\alpha+1}}{\alpha+1} C_{\alpha,0}^{\psi} = -7.61428 \times 10^6\,T - 14353.7\,T^2 + \cdots, \tag{74a}$$
$$\varepsilon = \sum_\alpha \frac{T^{\alpha+1}}{\alpha+1} C_{\alpha,0}^{\varepsilon} = -2.42138\,T + 2007.5\,T^2 + \cdots \tag{74b}$$

Terms with $\alpha \geq 3$ are negligible, in the sense that they are below 0.01 mas at 50 years from J2000. Note, as in Sect. 4.2.3, that we first computed the solution for the value of H_D of Roosbeek (1999), and updated the value of H_D so that the total precession rate of the full solution (solar, satellite and planet torques + geodetic precession) is consistent with the measured precession rate. For the solution expressed in terms of the right ascension and declination, we have, see Eqs. (24a, 24b):

$$\begin{aligned}\alpha &= -3.91248 \times 10^6\,T - 5096.0\,T^2 + \ldots \text{ (in mas)},\\ &= -1^\circ.08680\,T - 0^\circ.00142\,T^2 + \ldots,\end{aligned} \tag{75a}$$
$$\begin{aligned}\delta &= -2.22056 \times 10^6\,T - 5648.2\,T^2 + \ldots \text{ (in mas)},\\ &= -0^\circ.61682\,T - 0^\circ.00157\,T^2 + \ldots\end{aligned} \tag{75b}$$

For $j \geq 1$, the solution for the longitude and obliquity nutations has amplitudes given by (terms with $\alpha \geq 2$ are fully negligible, in the sense that they do not alter the amplitude

nutations before the third decimal)

$$\psi_j^{c/s} = \sum_\alpha T^\alpha \psi_{\alpha,j}^{c/s}, \tag{76a}$$

$$\varepsilon_j^{c/s} = \sum_\alpha T^\alpha \varepsilon_{\alpha,j}^{c/s}, \tag{76b}$$

with

$$\begin{pmatrix} \psi_{0,j}^c \\ \psi_{0,j}^s \\ \varepsilon_{0,j}^c \\ \varepsilon_{0,j}^s \end{pmatrix} = \frac{1}{\dot\varphi_j} \begin{pmatrix} -S_{0,j}^\psi \\ C_{0,j}^\psi \\ -S_{0,j}^\varepsilon \\ C_{0,j}^\varepsilon \end{pmatrix} + \frac{1}{\dot\varphi_j^2} \begin{pmatrix} C_{1,j}^\psi \\ S_{1,j}^\psi \\ C_{1,j}^\varepsilon \\ S_{1,j}^\varepsilon \end{pmatrix} + \cdots, \tag{76c}$$

$$\begin{pmatrix} \psi_{1,j}^c \\ \psi_{1,j}^s \\ \varepsilon_{1,j}^c \\ \varepsilon_{1,j}^s \end{pmatrix} = \frac{1}{\dot\varphi_j} \begin{pmatrix} -S_{1,j}^\psi \\ C_{1,j}^\psi \\ -S_{1,j}^\varepsilon \\ C_{1,j}^\varepsilon \end{pmatrix} + \cdots \tag{76d}$$

The first term in Eq. (76c) corresponds to the periodic nutation series as computed in Roosbeek (1999). The second term represents small alterations of the periodic nutation series. Equation (76d) is the nutation Poisson series. The series solution, for the updated value of H_D (0.00538017), is available at https://doi.org/10.24414/h5pn-7n71, for the three representations of the solution (longitude/obliquity, prograde/retrograde, right ascension/declination) defined in Sect. 3.2. Selected terms are presented in Tables 9 (periodic series) and 10 (Poisson series).

The periodic solution includes four terms of long period ($>$ 800 years, lines 40–43 of Table 9). About J2000, they would be perceived as secular terms with $\dot\Psi_{LP} = -0.002$ mas/yr and $\dot E_{LP} = -0.0006$ mas/yr by radioscience experiments spread between the seventies (e.g., Viking) and the coming years (e.g., LaRa). Compared to $\dot\Psi_S = -7578.28$ mas/yr and the future expected precision on the precession rate measurement (± 0.03 mas/yr), $\dot\Psi_{LP}$ is small. $\dot E_{LP}$ is small, but only four times smaller than $\dot E_S = -0.0024$ mas/yr. The other periodic terms have period $\lesssim$ 50 years and can be observed, if they are of detectable amplitude.

We add the geodetic precession and annual nutation (line 23 of Table 9) defined in Sect. 3.4.3 to the solar terms obtained above. We also add a semi-diurnal term (line 1 of Table 9), obtained after integration of the last terms of Eqs. (11a, 11b). We use

$$\delta H_D^{\rm tri} = 4\sqrt{C_{22}^2 + S_{22}^2}\frac{{\rm MR}^2}{C} = 0.000694106, \tag{77}$$

with the unnormalized gravity coefficients $C_{22} = -0.0000546304$ and $S_{22} = 0.0000315903$ (Konopliv et al. 2016) and $C/{\rm MR}^2$ from Eq. (70). The argument ϕ is defined as

$$\phi = 208^\circ.3654777 + \Omega_R t. \tag{78}$$

The J2000 value of ϕ is the sum of ϕ_0 and $\delta\phi_0$. $\phi_0 = 133^\circ.3848958$ is the rotation angle of the prime meridian measured from the node of Mars equator over the mean Mars orbit of J2000 (our IF), and obtained after transformation of the angle ϕ_0 of Konopliv et al. (2016) measured from the node of Mars equator over the mean Mars orbit of J980. $\delta\phi_0 = 74^\circ.9805819$ is the angle from the prime meridian to the axis of least inertia, obtained as $\frac{1}{2}\arctan S_{22}/C_{22}$.

Table 8 Mean orbital elements of Phobos and Deimos adapted from Jacobson et al. (2018) and Jacobson and Lainey (2014), to be used in the analytical solution of Eqs. (39a, 39b)

Parameter	Symbol (Unit)	Phobos	Deimos
$G\times$Mass	$G\mathcal{M}_P$ (km^3/s^2)	$(7.092 \pm 0.004) \times 10^{-4}$	$(0.962 \pm 0.028) \times 10^{-4}$
Semi-major axis	a_P (km)	9375	23458
Tilt between Mars equator and the local Laplace plane	τ (°)	0.009	0.889
Inclination with respect to the Laplace plane	i_p (°)	1.076	1.789
Node longitude J2000 with respect to the Laplace plane	$\Omega_P\vert_{J2000}$ (°)	122.079	11.614
Node longitude rate	$\dot{\Omega}_P$ (°/day)	-0.436	-0.018

The node longitude is expressed here with respect to the common node of the Laplace plane and mean equator of Mars over the orbit of Mars

4.3.2 Satellite terms

We inject the mean orbital elements of Phobos and Deimos from Jacobson and Lainey (2014), as given in Table 8, in the main terms of the analytical solution of Eqs. (39a, 39b) for the precession/nutations induced by the satellites. We obtain (in mas)

$$\Delta\psi = -0.235 \times 10^3\, T - 10.125 \sin\Omega_P, \tag{79a}$$
$$\Delta\varepsilon = -4.310 \cos\Omega_P, \tag{79b}$$

($\dot{\alpha} = -0.121$ mas/yr and $\dot{\delta} = -0.069$ mas/yr) for the motion induced by Phobos, and

$$\Delta\psi = -0.201 \times 10^3\, T - 3.532 \sin\Omega_D, \tag{80a}$$
$$\Delta\varepsilon = -1.503 \cos\Omega_D, \tag{80b}$$

($\dot{\alpha} = -0.103$ mas/yr and $\dot{\delta} = -0.059$ mas/yr) for the motion induced by Deimos. The node longitudes Ω_P and Ω_D, are the arguments N_{Ph} and N_{De} of the updated series:

$$N_{Ph} = 2.13055663363 - 2779.4193805084T, \tag{81a}$$
$$N_{De} = 0.20283841509 - 114.7466716724T. \tag{81b}$$

The updated solution is close (+3%) to the RMAN99 solution for Phobos torque. However, the updated solution for Deimos torque is significantly different (−20%), because the Deimos mass has been significantly revised by Jacobson and Lainey (2014). Note, as in Sect. 4.2.3, that we first computed the satellite terms for the value of H_D of Roosbeek (1999), and updated the value of H_D so that the total precession rate of the full solution is consistent with the measured precession rate.

4.3.3 Planetary terms

We integrate the AM Eqs. (12a, 12b). The planet coordinates in the equinox BF are given by

$$\begin{pmatrix} X_{Pl} \\ Y_{Pl} \\ Z_{Pl} \end{pmatrix} = \mathbf{R_x}(\varepsilon_0) \cdot \mathbf{R_z}(\theta_0) \cdot \mathbf{R_x}(i_0) \cdot \mathbf{R_z}(\Omega_0). \begin{pmatrix} x_{Pl} - x_M \\ y_{Pl} - y_M \\ z_{Pl} - z_M \end{pmatrix}, \tag{82}$$

with (x_M, y_M, z_M) and (x_{Pl}, y_{Pl}, z_{Pl}) as given in the VSOP2000 for the position of Mars and of the other planet in a reference frame attached to the ecliptic (Earth orbit) and equinox (ascending node of the Earth orbit on the Earth equator) at the J2000 epoch. They are given under the form of Eq. (58a), and we consider only $\alpha = 0$ here (no Poisson terms).

The distance d_{PlM} between Mars and another planet varies greatly with time, especially if their semi-major axes are close to each other. Therefore, it is difficult to obtain a convergent development for $1/d_{PlM}^{-5}$ such as in Eq. (62) from the VSOP2000 series for the rectangular coordinates. To obtain a workable expression for $1/d_{PlM}^{5}$, we therefore assume that the orbits of Mars and of the other planets are Keplerian and not inclined with respect to each other, and we use the mean orbital elements of Simon et al. (2013). We are entitled to neglect the mutual inclination, as we have seen that d_{PlM}^2 is independent from i_M and i_{Pl} at first order (Eq. 44a). Under those approximations, we have

$$d_{PlM}^2 = d_M^2 + d_{Pl}^2 - 2 d_M d_{Pl} \cos(\bar{\omega}_{Pl} + \nu_{Pl} - \bar{\omega}_M + \nu_M), \tag{83}$$

with $\bar{\omega} = \Omega + \omega$, and we develop $a_\alpha^5 d_{PlM}^{-5}$, with $a_\alpha = max(d_M, d_{Pl})$, to order 30 about $\alpha = \min(d_{Pl}/d_M, d_M/d_{Pl})$. Then, we replace $d_{M/Pl}$ and $\nu_{M/Pl}$ by developments correct up to the third order in $e_{M/Pl}$. This procedure, which can be seen as a more accurate extension of Eq. (45), ensures a good (for Saturn and Jupiter) or fair (for the Earth and Venus) accuracy of the semi-analytical solution obtained, compared to a numerical integration of the solution using the VSOP2000 series for $1/d_{PlM}^{-5}$ (absolute differences smaller than 0.001 mas for Jupiter and Saturn, relative differences smaller than 10% for the Earth and Venus).

After integration of the AM equations, the contributions of Jupiter, Saturn, Earth, Venus and Mercury to the variations rates in longitude and in obliquity can be expressed as:

$$\dot{\Psi}_{Pl} = -0.2223 - 0.0743 - 0.0097 - 0.0341 - 0.0015 = -0.342 \text{ mas/yr}, \tag{84a}$$

$$\dot{E}_{Pl} = \underbrace{-0.0063}_{\text{Jupiter}} \underbrace{-0.0002}_{\text{Saturn}} \underbrace{+0.0035}_{\text{Earth}} \underbrace{+0.0002}_{\text{Venus}} \underbrace{+0.0000}_{\text{Mercury}} = -0.003 \text{ mas/yr}, \tag{84b}$$

corresponding to $\dot{\alpha} = -0.179$ mas/yr and $\dot{\delta} = -0.098$ mas/yr. In addition, the direct effect of the planets causes 5 nutations terms (2 induced by Jupiter, 2 induced by the Earth, and one induced by Venus) above the chosen truncation level of 0.025 mas in amplitude (Table 9).

The planetary induced precession rate is larger in magnitude (+55%) than the one retained in RK79 (−0.22 mas/yr) and used in Konopliv et al. (2016), because we consider not only Jupiter, but also other planets of the solar system. Note, as in Sect. 4.2.3, that we first computed the planetary terms for the value of H_D of Roosbeek (1999), and updated the value of H_D so that the total precession rate of the full solution is consistent with the measured precession rate.

4.3.4 BMAN20RS: practical solution for Planetary Science

The BMAN20 solution for the orientation of Mars angular momentum axis in space includes secular and quadratic terms in longitude and obliquity, as well as 43 nutations terms with

Table 9 Selected periodic terms (main solar terms, satellite terms, …) of the BMAN20 nutations series, using the longitude/obliquity and prograde/retrograde representations defined in Sect. 3.2

j	Sa	Ju	Ma	Te	Ve	N_{Ph}	N_{De}	ϕ	$2\pi/f_j$ (d)	ψ_j^c (mas)	ψ_j^s (mas)	ε_j^c (mas)	ε_j^s (mas)	$\mathcal{P}_j$ (mas)	$\mathcal{R}_j$ (mas)
1 (SD)	0	0	0	0	0	0	0	2	0.513	0.000	0.110	−0.047	0.000	0.000	0.047
2	0	0	7	0	0	0	0	0	98.140	−0.102	0.085	0.040	0.048	0.059	0.003
3	0	0	6	0	0	0	0	0	114.497	−0.898	0.255	0.118	0.421	0.417	0.020
4	0	0	5	0	0	0	0	0	137.396	−6.292	−0.889	−0.429	2.942	2.839	0.134
5	0	0	4	0	0	0	0	0	171.745	−34.998	−21.766	−10.258	16.269	18.388	0.847
7	0	−3	11	−4	0	0	0	0	228.913	0.095	−0.031	−0.014	−0.044	0.044	0.002
8	0	0	3	0	0	0	0	0	228.993	−137.727	−201.016	−93.959	62.969	108.412	4.727
9	0	3	−5	4	0	0	0	0	229.074	0.063	−0.078	−0.036	−0.030	0.045	0.002
14	0	−3	10	−4	0	0	0	0	343.309	0.309	0.028	0.016	−0.140	0.137	0.005
15	−6	8	−5	0	2	0	0	0	343.489	0.075	−0.077	−0.034	−0.035	0.047	0.002
16	0	0	2	0	0	0	0	0	343.490	−221.944	−1113.768	−509.879	88.885	500.446	18.118
17	6	−8	9	0	−2	0	0	0	343.491	0.099	0.042	0.020	−0.045	0.047	0.002
18	0	3	−6	4	0	0	0	0	343.671	0.274	−0.144	−0.063	−0.127	0.137	0.005
23 (G)	0	0	1	0	0	0	0	0	686.980	0.229	0.516	0.000	0.000	0.120	0.120
24	0	0	1	0	0	0	0	0	686.980	−283.834	−480.044	47.897	11.969	102.595	137.356
27 (P)	0	0	0	0	0	−1	0	0	825.688	0.000	10.127	−4.310	0.000	0.000	4.310
30 (J)	0	−3	1	0	0	0	0	0	1310.238	0.018	−0.079	0.037	0.009	0.002	0.036
31 (J)	0	2	0	0	0	0	0	0	2166.295	−0.042	−0.187	−0.088	0.022	0.086	0.005
33 (E)	0	0	4	−2	0	0	0	0	2882.003	−0.012	−0.078	−0.029	0.006	0.032	0.002
35 (E)	0	0	2	−1	0	0	0	0	5764.006	−0.076	−0.129	0.006	0.001	0.030	0.034
37 (V)	0	0	−3	0	1	0	0	0	11987.226	0.034	−0.150	0.066	0.012	0.002	0.066
39 (D)	0	0	0	0	0	0	−1	0	20000.000	0.000	3.532	−1.503	0.000	0.000	1.503
40	5	−2	0	0	0	0	0	0	322618.691	−0.373	0.112	−0.143	0.076	0.127	0.104
41	0	−3	8	−4	0	0	0	0	651385.029	1.003	0.284	−0.002	0.015	0.215	0.229
42	5	4	−16	8	0	0	0	0	3.41836×10^7	0.131	0.052	−0.008	−0.015	0.036	0.025
43	−6	8	−7	0	2	0	0	0	1.32273×10^8	0.278	−0.212	−0.029	−0.024	0.093	0.056

The full solution is available at https://doi.org/10.24414/h5pn-7n71. The arguments $Sa, \ldots, Ve$ are given in Eqs. (72a–72e), ϕ is given in Eq. (78), and N_{Ph} and N_{De} are given in Eqs. (81a–81b). The table contains terms which have prograde and/or retrograde amplitudes larger than 0.025 mas. The first seven main solar terms, satellites terms (Phobos, Deimos), and direct planetary terms (Jupiter, Earth, and Venus) are highlighted in blue, gray, and pink, respectively. The geodetic annual term is included in line 23. One semi-diurnal term related to triaxiality is also included (line 1)

pro and or retrograde amplitude larger than 0.025 mas (36 induced by the Sun, one of them being the geodetic annual nutation, 1 by Phobos, 1 by Deimos, 2 by Jupiter, 2 by the Earth, and 1 by Venus), of which 4 terms (the first main solar terms) have amplitudes varying with time (see Tables 9, 10). This truncation criterion is sufficient for the interpretation of the RISE and LaRa radioscience experiment. Recent simulations (Dehant et al. 2020; Péters et al. 2020; Le Maistre et al. 2020) suggest that only the secular variation in longitude, the secular variations in obliquity (if as large as about −0.2 mas/yr, which is not the case in the BMAN20 solution, where $\dot{E} \simeq -0.006$ mas/yr due to the Sun and the planets, including the long period nutation terms), and the largest nutations terms can influence the transponders' radio signal in a detectable way.

A higher accuracy of the theoretical rigid precession/nutation model than the accuracy of the observation is needed since terms that can observationally not be identified separately can contaminate other signals. Over short times scales such as the duration of the RISE and LaRa mission, the quadratic terms in longitude and obliquity (see Eqs. 74a, 74b) will be perceived as secular variations (− 0.632 mas/yr and + 0.088 mas/yr, in longitude and obliquity, about J2022), introducing a bias on the determination of H_D. Similarly, the Poisson nutation terms will be perceived as part of the periodic nutation terms (with a periodic contribution of 1.245 mas from the Poisson cosine annual term in longitude in J2022, for instance), and some terms with periods very close to the period of the main nutation terms will be perceived

Table 10 Poisson terms of the BMAN20 nutations series

j	*Sa*	*Ju*	*Ma*	*Te*	*Ve*	N_{Ph}	N_{De}	ϕ	$2\pi/f_j$ (d)	ψ_j^c (mas) ($T\times$)	ψ_j^s (mas) ($T\times$)	ε_j^c (mas) ($T\times$)	ε_j^s (mas) ($T\times$)	$\mathcal{P}_j$ (mas) ($T\times$)	$\mathcal{R}_j$ (mas) ($T\times$)
From Poisson series in the ephemerides															
5	0	0	4	0	0	0	0	0	171.745	2.588	− 6.004	− 2.779	− 1.218	2.909	0.126
8	0	0	3	0	0	0	0	0	228.993	14.091	− 13.982	− 6.243	− 6.509	8.734	0.294
16	0	0	2	0	0	0	0	0	343.490	4.166	− 9.296	− 2.159	− 0.166	3.208	1.206
24	0	0	1	0	0	0	0	0	686.980	49.090	− 24.520	1.735	− 3.181	12.800	10.747
From $\dot{\theta}$ (mean precession rate in longitude)															
5	0	0	4	0	0	0	0	0	171.745	− 1.609	2.552	1.200	0.757	1.351	0.067
8	0	0	3	0	0	0	0	0	228.993	− 14.736	9.875	4.645	6.932	7.947	0.397
16	0	0	2	0	0	0	0	0	343.490	− 79.966	13.940	6.557	37.615	36.366	1.816
24	0	0	1	0	0	0	0	0	686.980	7.512	1.877	0.885	− 3.532	3.469	0.173
Sum of Poisson series and $\dot{\theta}$ contributions															
5	0	0	4	0	0	0	0	0	171.745	0.980	− 3.452	− 1.579	− 0.461	1.586	0.059
8	0	0	3	0	0	0	0	0	228.993	− 0.645	− 4.107	− 1.597	0.423	1.709	0.106
16	0	0	2	0	0	0	0	0	343.490	− 75.799	4.644	4.398	37.449	35.002	2.862
24	0	0	1	0	0	0	0	0	686.980	56.602	− 22.643	2.620	− 6.713	15.798	10.634

See legend of Table 9 for information about the representation of the solution and the definition of the arguments. T is in thousand years past J2000. See also https://doi.org/10.24414/h5pn-7n71

as contribution to those main terms, introducing bias in the determination of Mars' interior. By using in combination the data from older missions (e.g., the Viking missions in the late seventies) with the RISE/LaRa data, the ambiguity between the secular and quadratic terms could be alleviated, and the quadratic terms detected, but only the recent data will bear information about nutations, since the accuracy of the older missions in the determination of nutation amplitudes is weak. If only recent data are used, a correction for the "secular" effect of the quadratic term in longitude should be introduced in Eq. (69) before determining H_D.

We therefore provide a modified version of the solution (named hereafter BMAN20 for Radio-Science, or **BMAN20RS**) which reproduces at best the behavior of the BMAN20 solution, but groups different terms (main periodic terms, Poisson terms, and periodic terms of period close to the period of the main periodic terms) into a more limited subset of nutation terms that can be observed and identified by RISE and LaRa. Discarding $\dot{E}$, BMAN20RS solution writes (in mas, and T is the time measured in thousands of years from J2000)

$$\psi = \psi_0 - (7.6083 \pm 0.0021)10^6\, T - (14353.7 \pm 4.0)T^2 + \Delta\psi, \tag{85a}$$

$$\varepsilon = \varepsilon_0 + (2007.5 \pm 0.6)\, T^2 + \Delta\varepsilon, \tag{85b}$$

$$\alpha = \alpha_0 - (3.90940 \pm 0.0011)10^6\, T - (5096.0 \pm 1.4)\, T^2 + \Delta\alpha, \tag{85c}$$

$$\delta = \delta_0 - (2.21882 \pm 0.0006)10^6\, T - (5648.2 \pm 1.6)\, T^2 + \Delta\delta. \tag{85d}$$

The periodic terms $\Delta\psi$, $\Delta\varepsilon$, $\Delta\alpha$, $\Delta\delta$ are given in Table 11. Table 11 also includes the pro/retrograde representation of the periodic terms. The J2000 epoch values are

$$\psi_0 = 35^\circ.4975258 \pm 0^\circ.0000043, \tag{86a}$$

$$\varepsilon_0 = 25^\circ.1918197 \pm 0^\circ.0000026, \tag{86b}$$

$$\alpha_0 = 317^\circ.6811155 \pm 0^\circ.0000037, \tag{86c}$$

$$\delta_0 = 52^\circ.8863525 \pm 0^\circ.0000023, \tag{86d}$$

see Sect. 3.4.3. The uncertainties on α_0 and δ_0 are obtained as in Eqs. (24a, 24b) from the uncertainties on ε_0 and θ_0 taken from Konopliv et al. (2016). The uncertainty on the other terms of the solution is $\pm 0.03\%$ and mainly results from the uncertainty on the scaling factor H_D, which results itself from the uncertainty of $\pm 0.03\%$ on the measured precession rate by Konopliv et al. (2016). The uncertainties are not indicated in Table 11, for the sake of conciseness. Only the geodetic term is not affected by this uncertainty, as it does not depend on H_D.

The periodic terms have been constructed as follows. Since the expected precision on the nutation amplitude measurements with RISE and LaRa is a few mas (Dehant et al. 2020; Péters et al. 2020; Le Maistre et al. 2020), only the satellite terms and the largest main solar terms are selected. The selected term with the smallest amplitude is the 6th-annual term (0.9 mas in longitude, likely just below the detection limit). The satellite terms are taken without modification in the modified solution. The period of the main solar terms are harmonics of the revolution period of Mars. The 5th-annual and 6th-annual terms are taken from BMAN20 without modification. For the quarter, ter, semi, and annual terms, the corresponding BMAN20 terms are modified to take into account the Poisson series and other terms of very close periods which cannot be distinguished from the main terms by the radioscience experiments.

The annual term In the longitude/obliquity representation, we take the main annual solar term (line 24 in Table 9) to which we add the Poisson annual term (Table 10) evaluated at J2022 (JD2459581.0), the average epoch of the RISE and LaRa mission duration, to obtain the modified annual term (in mas):

Table 11 Periodic terms of the BMAN20RS nutations series for the angular momentum axis, using the three representations of the solution (longitude/obliquity, prograde/retrograde, right ascension/declination) defined in Sect. 3.2

j	Ma	N_{Ph}	N_{De}	$2\pi/f_j$ (d)	ψ_j^c (mas)	ψ_j^s (mas)	ε_j^c (mas)	ε_j^s (mas)	$\mathcal{P}_j$ (mas)	$\mathcal{R}_j$ (mas)	π_j (°)	ρ_j (°)	α_j^c (mas)	α_j^s (mas)	δ_j^c (mas)	δ_j^s (mas)
1	6	0	0	114.497	− 0.898	0.255	0.118	0.421	0.417	0.020	168.343	346.409	− 0.327	0.609	− 0.348	− 0.232
2	5	0	0	137.396	− 6.292	− 0.889	− 0.429	2.942	2.839	0.134	148.997	326.401	− 3.720	2.883	− 1.523	− 2.402
3	4	0	0	171.745	− 34.976	− 21.842	− 10.293	16.259	18.398	0.847	129.570	305.762	− 29.659	7.239	− 2.703	− 18.213
4	3	0	0	228.993	− 137.902	− 200.996	− 93.949	62.965	108.424	4.708	110.432	283.246	− 177.535	− 31.783	28.216	− 104.481
5	2	0	0	343.490	− 224.053	− 1113.578	− 509.777	89.718	500.516	18.113	91.524	251.895	− 693.967	− 470.322	305.984	− 390.106
6	1	0	0	686.980	− 282.589	− 480.543	47.955	11.822	102.435	137.404	125.587	108.681	− 90.752	− 233.496	− 117.343	− 148.753
7 (G)	1	0	0	686.980	0.229	0.516	0.000	0.000	0.120	0.120	289.374	289.374	0.118	0.265	0.067	0.151
8 (P)	0	− 1	0	825.688	0.000	10.127	− 4.310	0.000	0.000	4.310	0.000	147.928	− 4.894	5.203	3.140	2.953
9 (D)	0	0	− 1	20000.000	0.000	3.532	− 1.503	0.000	0.000	1.503	0.000	258.378	− 1.707	1.815	1.095	1.030

The argument Ma is given in Eq. (72c). N_{Ph} and N_{De} are given in Eqs. (81a, 81b). BMAN20RS solution is valid about J2022, and can be used to interpret RISE and LaRa measurements. See also https://doi.org/10.24414/h5pn-7n71

$$\Delta\psi = -282.589\cos Ma - 480.543\sin Ma, \tag{87a}$$
$$\Delta\varepsilon = 47.955\cos Ma + 11.822\sin Ma. \tag{87b}$$

The difference with the main annual term of BMAN20 is 1 mas in longitude and 0.1 mas in obliquity. We keep the geodetic annual nutation separated from the modified annual term in the BMAN20RS solution, as it is not proportional to H_D, does not depend on the internal structure of Mars and therefore must not be multiplied by transfer functions in order to interpret radioscience data.

The semi-annual term We consider the main semi-annual solar term (line 16 in Table 9) and the Poisson semi-annual term (Table 10) evaluated at J2022, but also the 4 small solar terms of similar periods (lines 14, 15, 17, and 18 in Table 9). We first rewrite these four terms so that their sine and cosine phases vanish for t = J2022 (this ensures the best match between the exact and approximated terms). For instance, for line 15 in Table 9, in longitude, we obtain (amplitudes in mas, phases in radian)

$$\Delta\psi = 0.075\cos(-25.113 + 6.68124t) - 0.077\sin(-25.113 + 6.68124t) \tag{88a}$$
$$= -0.106\cos(6.68124(t - 22.0014)) + 0.017\sin(6.68124(t - 22.0014)), \tag{88b}$$

with t, the time in years from J2000. Then, we approximate the frequency by the semi-annual frequency ($2n$, with $n = \dot{M}a$):

$$\Delta\psi \simeq -0.106\cos(2n(t - 22.0014)) + 0.017\sin(2n(t - 22.0014)). \tag{88c}$$

After some trigonometric manipulation, we then obtain

$$\Delta\psi \simeq 0.038\cos 2Ma + 0.101\sin 2Ma. \tag{88d}$$

We proceed in the same way for the four terms, both in longitude and obliquity, and add them to the main and Poisson terms, to obtain the modified term presented in Table 11. The difference with the main semi-annual term of BMAN20 is 2 mas in longitude and 1 mas in obliquity.

The ter-annual term The procedure is similar to the one used for the semi-annual term. We consider the main term (line 8 of Table 9), the Poisson term (Table 10), and the two terms of similar periods (lines 7 and 9 in Table 9). The difference with the main ter-annual term of BMAN20 is of 0.20 mas in longitude and 0.04 mas in obliquity.

The quarter-annual term We only need to consider the main term (line 5 of Table 9) and the Poisson term (Table 10), just as we did for the annual term. The difference with the main quarter-annual term of BMAN20 is of 0.07 mas in longitude and 0.03 mas in obliquity.

5 IAU standard model for Mars spin axis position

Differently from previous reports, the latest IAU standard model for the right ascension (α) and the declination (δ) of Mars spin axis includes the periodic variations of the angles along with the traditional secular terms (Archinal et al. 2018). In this section, we explain why we consider that the current IAU standard model has no added practical relevance compared to the previous standard model.

First, the current IAU model is a Fourier series fitted by Kuchynka et al. (2014) to an α/δ time series derived from the ψ/ε nutation model of Konopliv et al. (2006) (see also Jacobson 2010; Jacobson et al. 2018). Inherently to their methods, such solutions obtained from the fits include a long period (about 70, 000 years) terms in α and in δ that have no physical

significance and that alter the definition of the epoch α (317°.269 instead of 317°.681) and above all of the epoch δ (54°.432 instead of 52°.886). In addition, the periods of the terms in α/δ obtained with the FFT approach are not exactly the same. These differences have no physical origin. It is easier and more accurate to derive an α/δ model from a given ψ/ε nutation model by considering the geometrical transformation as described in Sect. 3.4.3.

Second, the ψ/ε nutation model of Konopliv et al. (2006) is derived from the ψ/ε rigid nutation model of RK79, which was built for the figure axis and not for the spin axis (see Sect. 3.7), introducing errors of the order of a few mas. Besides, RK79 and Konopliv et al. (2006) models do not include the nutation terms induced by Phobos and Deimos, which have amplitudes between 1 and 10 mas. They also do not take into account the complex orbital dynamics of Mars, perturbed by the other planets of the solar system. The solution BMAN20RS for a rigid Mars defined above would be a more relevant basis to define a α/δ standard model including periodic terms, assuming that Mars behaves rigidly.

Third, IAU practice is to provide α/δ models without giving uncertainties, assuming that the provided angle values are representative of their "true" values. Kuchynka's α/δ and Konopliv's ψ/ε models are based on measurements for the epoch values of the angles and their secular variations and on models for the periodic part. This computed periodic part is based on a rigid nutation model (RK79) altered by the action of a liquid core, which is modeled by transfer functions depending on the liquid core amplification factor F and on the free core nutation period T_{FCN} (see Eq. 16 of Konopliv et al. 2006 or Eq. 12 of Dehant et al. 2020). The nutation model so obtained by Konopliv et al. (2006) considers unique values for the nutation parameters (i.e., $F = 0.07$ and $T_{FCN} = -240$ days). However, the uncertainties in nutation amplitudes (either in ψ/ε or in α/δ) brought by the uncertainties on F and T_{FCN} are so large that it is currently pointless to propose one specific value for the nutation amplitudes that the users would mistakenly assume realistic/representative.

This being said, a IAU model with relevant periodic terms shall be proposed after RISE and LaRa experiments, which will determine the nutation amplitudes and the core parameters.

6 Discussion and conclusions

The precession and nutations of Mars spin axis will be estimated to an unprecedented accuracy with the radioscience experiments RISE and LaRa (Folkner et al. 2018; Dehant et al. 2020), allowing to confirm the presence of a liquid core and to constrain Mars' interior.

Given the expected precision on the determination of the nutation amplitudes (a few mas, Dehant et al. 2020; Péters et al. 2020; Le Maistre et al. 2020) and the modifications of the amplitudes due to the liquid core and tidal deformations (from a few mas to a few tens of mas, depending on the core dimensions, Le Maistre et al. 2012, 2020), the existing models for the nutation of a rigid Mars are not suitable for the interpretation of radioscience measurements, due to a lack of accuracy and/or inappropriate modeling approximations. For instance, we have seen that the solution RMAN99 (Roosbeek Martian Analytical Nutations 1999) of Roosbeek (1999) lacks of internal accuracy due to a too loose computational procedure, whereas the solution of Reasenberg and King (1979) does not include the effect of Phobos and Deimos and concerns the axis of figure and not the spin axis.

As the use of those existing models can introduce systematic errors in the determination of the core properties, we have developed a new model, based on the method of Roosbeek (1999) and an adequate computational procedure. We have included the effect of different forcings (by the Sun, Phobos and Deimos, and the other planets of the solar system). We

have also included the geodetic precession and nutations in the solution. This new model, called BMAN20 (Baland Martian Analytical Nutations 2020), is based on semi-analytical developments for the solar and planetary torques, and on analytical solutions for the effect of Phobos and Deimos and the geodetic precession/nutations. The uncertainty on BMAN20 solution derives in a one to one way from the uncertainty in H_D, except for the geodetic contribution. A modified version of the solution, more suited for interpretation of radioscience data, has been derived alongside. Using our new precession/nutation model, we have updated the values of the scaling factor H_D ($0.00538017 \pm 0.00000148$) determined from the measured rate of precession in longitude rate ($\dot{\Psi} = -7608.3 \pm 2.1$ mas/yr, Konopliv et al. 2016), and of the normalized polar moment of inertia $\frac{C}{MR^2}$ ($= 0.36367 \pm 0.00010$). Finally, we have questioned the relevance of the current IAU standard for the orientation of the spin axis of Mars which is partially based on assumptions about the unknown characteristics of the core of Mars.

The RMAN99 recomputed (Table 6), BMAN20 (Tables 9, 10), and BMAN20RS (Table 11) series are available at https://doi.org/10.24414/h5pn-7n71.

Acknowledgements We thank Fabian Roosbeek and Georges Carpentier for helping us to understand the computational procedure of RMAN99. We thank Michael Efroimsky and an anonymous reviewer for their constructive comments and suggestions that have helped to improve our paper. The research leading to these results has received funding from the Belgian PRODEX program managed by the European Space Agency in collaboration with the Belgian Federal Science Policy Office.

Compliance with ethical standards

Conflict of interest The authors declare that they have no conflict of interest.

References

Archinal, B.A., Acton, C.H., A'Hearn, M.F., Conrad, A., Consolmagno, G.J., Duxbury, T., et al.: Report of the IAU Working Group on cartographic coordinates and rotational elements: 2015. Celest. Mech. Dyn. Astron. **130**, 22 (2018). https://doi.org/10.1007/s10569-017-9805-5

Borderies, N.: Theory of Mars rotation in Euler angles. Astron. Astrophys. **82**, 129–141 (1980)

Borderies, N., Balmino, G., Castel, L., Moynot, B.: Study of Mars dynamics from lander tracking data analysis. Moon Planets **22**, 191–200 (1980). https://doi.org/10.1007/BF00898430

Bouquillon, S., Souchay, J.: Precise modeling of the precession-nutation of Mars. Astron. Astrophys. **345**, 282–297 (1999)

Bretagnon, P.: Theorie du mouvement de l'ensemble des planetes (VSOP82). Astron. Astrophys. **114**, 278 (1982)

Bretagnon, P., Francou, G.: Planetary theories in rectangular and spherical variables—VSOP 87 solutions. Astron. Astrophys. **202**, 309–315 (1988)

Chapront-Touze, M.: Orbits of the Martian satellites from ESAPHO and ESADE theories. Astron. Astrophys. **240**, 159–172 (1990)

Davies, M.E., Abalakin, V.K., Bursa, M., Hunt, G.E., Lieske, J.H., Morando, B., et al.: Report of the IAU/IAG/COSPAR working group on cartographic coordinates and rotational elements of the planets and satellites—1988. Celes. Mech. Dyn. Astron. **46**, 187–204 (1989). https://doi.org/10.1007/BF00053048

Defraigne, P., Dehant, V., Pâquet, P.: Link between the retrograde-prograde nutations and nutations in obliquity and longitude. Celest. Mech. Dyn. Astron. **62**(4), 363–376 (1995). https://doi.org/10.1007/BF00692286

Defraigne, P., de Viron, O., Dehant, V., Van Hoolst, T., Hourdin, F.: Mars rotation variations induced by atmosphere and ice caps. J. Geophys. Res. **105**(E10), 24563–24570 (2000). https://doi.org/10.1029/1999JE001227

Dehant, V., Mathews, P.M.: Precession, Nutation and Wobble of the Earth. Cambridge University Press, Cambridge (2015)

Dehant, V., Defraigne, P., Van Hoolst, T.: Computation of Mars' transfer functions for nutations, tides and surface loading. Phys. Earth Planet. Inter. **117**(1–4), 385–395 (2000). https://doi.org/10.1016/S0031-9201(99)00108-9

Dehant, V., de Viron, O., Karatekin, O., van Hoolst, T.: Excitation of Mars polar motion. Astron. Astrophys. **446**(1), 345–355 (2006). https://doi.org/10.1051/0004-6361:20053825

Dehant, V., Le Maistre, S., Baland, R.M., Bergeot, N., Karatekin, Ö., Péters, M.J., et al.: The radio-science LaRa instrument onboard ExoMars 2020: to investigate the rotation and interior of Mars. Planet. Space Sci. (2020). https://doi.org/10.1016/j.pss.2019.104776

Fienga, A., Laskar, J., Kuchynka, P., Manche, H., Desvignes, G., Gastineau, M., et al.: The INPOP10a planetary ephemeris and its applications in fundamental physics. Celest. Mech. Dyn. Astron. **111**(3), 363–385 (2011). https://doi.org/10.1007/s10569-011-9377-8

Folkner, W.M., Kahn, R.D., Preston, R.A., Yoder, C.F., Standish, E.M., Williams, J.G., et al.: Mars dynamics from Earth-based tracking of the Mars Pathfinder lander. J. Geophys. Res. **102**(E2), 4057–4064 (1997a). https://doi.org/10.1029/96JE02125

Folkner, W.M., Yoder, C.F., Yuan, D.N., Standish, E.M., Preston, R.A.: Interior structure and seasonal mass redistribution of Mars from radio tracking of Mars pathfinder. Science **278**, 1749 (1997b). https://doi.org/10.1126/science.278.5344.1749

Folkner, W.M., Dehant, V., Le Maistre, S., Yseboodt, M., Rivoldini, A., Van Hoolst, T., et al.: The rotation and interior structure experiment on the InSight mission to Mars. Space Sci. Rev. **214**, 100 (2018). https://doi.org/10.1007/s11214-018-0530-5

Fukushima, T.: Geodesic nutation. Astron. Astrophys. **244**(1), L11 (1991)

Fukushima, T.: A new precession formula. Astron. J. **126**(1), 494–534 (2003). https://doi.org/10.1086/375641

Groten, E., Molodenski, S.M., Zharkov, V.N.: On the theory of Mars' forced nutation. Astron. J. **111**, 1388 (1996). https://doi.org/10.1086/117885

Hilton, J.L.: The motion of Mars' pole. I—rigid body precession and nutation. Astron. J. **102**, 1510–1527 (1991). https://doi.org/10.1086/115977

Hilton, J.L.: The motion of Mars' pole. II. The effect of an elastic mantle and a liquid core. Aastron. J. **103**, 619 (1992). https://doi.org/10.1086/116090

Jacobson, R.A.: The orbits and masses of the Martian satellites and the libration of Phobos. Astron. J. **139**(2), 668–679 (2010). https://doi.org/10.1088/0004-6256/139/2/668

Jacobson, R.A., Lainey, V.: Martian satellite orbits and ephemerides. Planet. Space Sci. **102**, 35–44 (2014). https://doi.org/10.1016/j.pss.2013.06.003

Jacobson, R.A., Konopliv, A.S., Park, R.S., Folkner, W.M.: The rotational elements of Mars and its satellites. Planet. Space Sci. **152**, 107–115 (2018). https://doi.org/10.1016/j.pss.2017.12.020

Khan, A., Liebske, C., Rozel, A., Rivoldini, A., Nimmo, F., Connolly, J.A.D., et al.: A geophysical perspective on the bulk composition of Mars. J. Geophys. Res. (Planets) **123**(2), 575–611 (2018). https://doi.org/10.1002/2017JE005371

Konopliv, A.S., Yoder, C.F., Standish, E.M., Yuan, D.-N., Sjogren, W.L.: A global solution for the Mars static and seasonal gravity, Mars orientation, Phobos and Deimos masses, and Mars ephemeris. Icarus **182**, 23–50 (2006). https://doi.org/10.1016/j.icarus.2005.12.025

Konopliv, A.S., Park, R.S., Folkner, W.M.: An improved JPL Mars gravity field and orientation from Mars orbiter and lander tracking data. Icarus **274**, 253–260 (2016). https://doi.org/10.1016/j.icarus.2016.02.052

Konopliv, A.S., Asmar, S.W., Folkner, W.M., Karatekin, Ö., Nunes, D.C., Smrekar, S.E., et al.: Mars high resolution gravity fields from MRO, Mars seasonal gravity, and other dynamical parameters. Icarus **211**(1), 401–428 (2011). https://doi.org/10.1016/j.icarus.2010.10.004

Kuchynka, P., Folkner, W.M., Konopliv, A.S., Parker, T.J., Park, R.S., Le Maistre, S., et al.: New constraints on Mars rotation determined from radiometric tracking of the Opportunity Mars Exploration Rover. Icarus **229**, 340–347 (2014). https://doi.org/10.1016/j.icarus.2013.11.015

Laskar, J., Robutel, P.: Stability of the planetary three-body problem. I. Expansion of the planetary Hamiltonian. Celest. Mech. Dyn. Astron. **62**(3), 193–217 (1995). https://doi.org/10.1007/BF00692088

Le Maistre, S.: The Rotation of Mars and Phobos from Earth-based Radio-tracking Observations of a Lander. PhD thesis. Université Catholique de Louvain (2013)

Le Maistre, S., Rosenblatt, P., Rivoldini, A., Dehant, V., Marty, J.-C., Karatekin, O.: Lander radio science experiment with a direct link between Mars and the Earth. Planet. Space Sci. **68**, 105–122 (2012). https://doi.org/10.1016/j.pss.2011.12.020

Le Maistre, S., Dehant, V., Marty, J.-C.: Mars nutation estimates from radio-tracking of landed missions prior InSight and ExoMars 2020. In: European Planetary Science Congress, 12: EPSC2018-1238 (2018)

Le Maistre, S., Péters, M.J., Marty, J.-C., Dehant, V.: On the impact of the operational and technical characteristics of the LaRa experiment on the determination of Mars' nutation. Planet. Space Sci. **180**, 104766 (2020). https://doi.org/10.1016/j.pss.2019.104766
Lowrie, W.: A Student's Guide to Geophysical Equations. Cambridge University Press, Cambridge (2011)
Lyttleton, R.A., Cain, D.L., Liu, A.S.: Nutation of Mars. Technical report (1979)
Mathews, P.M., Buffett, B.A., Herring, T.A., Shapiro, I.I.: Forced nutations of the earth: influence of inner core dynamics. I—Theory. II—numerical results and comparisons. III—very long interferometry data analysis. J. Geophys. Res. **96**, 8219–8257 (1991). https://doi.org/10.1029/90JB01955
McCarthy, D.D.: IERS Conventions (1996). IERS Technical Note 21, pp. 1–95 (1996)
Moisson, X., Bretagnon, P.: Analytical planetary solution VSOP2000. Celest. Mech. Dyn. Astron. **80**, 205–213 (2001)
Murray, C.D., Dermott, S.F.: Solar System Dynamics. Cambridge University Press, Cambridge (1999)
Newman, W.I.: Rotational kinematics and torques for triaxial bodies. Icarus **223**(1), 615–618 (2013). https://doi.org/10.1016/j.icarus.2012.12.023
Péters, M.J., Le Maistre, S., Yseboodt, M., Marty, J.C., Rivoldini, A., Van Hoolst, T., et al.: LaRa after RISE: expected improvement in the rotation and interior models. Planet. Space Sci. (2020). https://doi.org/10.1016/j.pss.2019.104745
Reasenberg, R.D., King, R.W.: The rotation of Mars. J. Geophys. Res. **84**, 6231–6240 (1979). https://doi.org/10.1029/JB084iB11p06231
Rivoldini, A., Van Hoolst, T., Verhoeven, O., Mocquet, A., Dehant, V.: Geodesy constraints on the interior structure and composition of Mars. Icarus **213**, 451–472 (2011). https://doi.org/10.1016/j.icarus.2011.03.024
Roosbeek, F.: Analytical developments of rigid Mars nutation and tide generating potential series. Celest. Mech. Dyn. Astron. **75**, 287–300 (1999)
Roosbeek, F., Dehant, V.: RDAN97: An analytical development of rigid Earth nutation series using the torque approach. Celest. Mech. Dyn. Astron. **70**(4), 215–253 (1998). https://doi.org/10.1023/A:1008350710849
Sasao, T., Okubo, S., Saito, M.: A simple theory on dynamical effects of stratified fluid core upon nutational motion of the Earth. In Duncombe, R.L. (ed.) Nutation and the Earth's Rotation, volume 78 of IAU Symposium, p. 165 (1980)
Simon, J.L., Bretagnon, P., Chapront, J., Chapront-Touze, M., Francou, G., Laskar, J.: Numerical expressions for precession formulae and mean elements for the Moon and the planets. Astron. Astrophys. **282**, 663–683 (1994)
Simon, J.-L., Francou, G., Fienga, A., Manche, H.: New analytical planetary theories VSOP2013 and TOP2013. Astron. Astrophys. **557**, A49 (2013). https://doi.org/10.1051/0004-6361/201321843
Sinclair, A.T.: The motions of the satellites of Mars. Mon. Not. R. Astron. Soc. **155**, 249 (1972). https://doi.org/10.1093/mnras/155.3.249
Standish Jr., E.M.: Orientation of the JPL Ephemerides, DE 200/LE 200, to the dynamical equinox of J 2000. Astron. Astrophys. **114**, 297–302 (1982)
Standish Jr., E.M., Newhall, X., Williams, J., Folkner, W.: JPL Interoffice Memorandum **314**, 10 (1995)
Van den Acker, E., Van Hoolst, T., de Viron, O., Defraigne, P., Forget, F., Hourdin, F., et al.: Influence of the seasonal winds and the CO_2 mass exchange between atmosphere and polar caps on Mars' rotation. J. Geophys. Res. (Planets) **107**(E7), 5055 (2002). https://doi.org/10.1029/2000JE001539
Ward, W.R.: Climatic variations on Mars: 1. Astronomical theory of insolation. J. Geophys. Res. **79**(24), 3375 (1974). https://doi.org/10.1029/JC079i024p03375
Woolard, E.W.: Theory of the rotation of the earth around its center of mass. In: Astronomical Papers Prepared for the Use of the American Ephemeris and Nautical Almanac, vol. 15, p. 1 (1953)
Yoder, C.F., Konopliv, A.S., Yuan, D.N., Standish, E.M., Folkner, W.M.: Fluid core size of Mars from detection of the solar tide. Science **300**, 299–303 (2003). https://doi.org/10.1126/science.1079645